Research Square

Preprints are preliminary reports that have not undergone peer review.
They should not be considered conclusive, used to inform clinical practice,
or referenced by the media as validated information.

A social-semantic-working-memory account for two canonical language areas

Guangyao Zhang
Institute of Psychology, Chinese Academy of Sciences
Yangwen Xu
University of Trento
Xiuyi Wang
Institute of Psychology, Chinese Academy of Sciences
Jixing Li
City University of Hong Kong
Weiting Shi
Institute of Psychology, Chinese Academy of Sciences
Yanchao Bi
Beijing Normal University
Nan Lin (linn@psych.ac.cn)
Institute of Psychology, Chinese Academy of Sciences

Article

Keywords:

Posted Date: February 17th, 2023

DOI: https://doi.org/10.21203/rs.3.rs-2537489/v1

License: This work is licensed under a Creative Commons Attribution 4.0 International License.
Read Full License

Abstract

Language and social cognition are traditionally studied as separate cognitive domains, yet accumulative studies reveal overlapping neural correlates at the left ventral temporoparietal junction (vTPJ) and lateral anterior temporal lobe (lATL), which have been attributed to sentence processing and social concept activation. We propose a common cognitive component underlying both effects -- social-semantic working memory. We confirmed two key predictions of our hypothesis using fMRI: First, the left vTPJ and lATL showed sensitivity to sentences only when the sentences conveyed social meaning.; second, these regions showed persistent social-semantic-selective activity after the linguistic stimuli disappeared. We additionally found that both regions were sensitive to the socialness of nonlinguistic stimuli and were more tightly connected with the social-semantic-processing areas than with the sentence-processing areas. The converging evidence indicates the social-semantic-working-memory function of the left vTPJ and lATL and challenges the general-semantic and/or syntactic accounts for the neural activity of these regions.

Introduction

Language and social cognition are two fundamental abilities of the human species. They are deeply interrelated with each other in cognitive development (de Villiers, 2007; Richardson et al., 2020), daily communication (Scott, 2019), and evolution (Dunbar, 2004). At the brain level, overlaps of regions underlying language and social cognition have been found in the left ventral temporoparietal junction (vTPJ; consisting of the ventral portion of the angular gyrus and its adjacent temporal cortex) and lateral anterior temporal lobe (lATL) (Bzdok et al., 2016; Mar, 2011; Mellem et al., 2016). Understanding the function of these regions will indicate how the language and social cognition are associated with each other in the brain.

In the field of social neuroscience, the left vTPJ and lATL have been found to be involved in multiple social cognitive tasks (Diveica et al., 2021; Mar, 2011; Schurz et al., 2021). Recent studies have indicated that these regions may support a very basic component of social cognition, that is, social concept representation and processing (Binney & Ramsey, 2020; Pexman et al., 2022; Arioli et al., 2021; Lin et al., 2020; Zhang et al., 2022). These regions are sensitive to a wide range of social concepts (concepts associated with people and their interactions), including traits (e.g., brave; Zahn et al., 2007), mental states (e.g., distrust; Tamir et al., 2016), stereotypes (e.g., women; Contreras et al., 2012), social backgrounds (e.g., having a good salary, Saxe & Wexler, 2005), social actions (e.g., chase; Lin et al., 2015; 2018a; Spunt et al., 2016), and social artifacts (e.g., telephone; Lin et al., 2019).

In the field of language neuroscience, the left vTPJ and lATL have both been found to be critical for sentence processing. Lesions in these regions can damage sentence comprehension (Dronkers et al., 2004). Neuroimaging studies found that, in both regions, sentences induce stronger activation than word lists or other unintelligible linguistic stimuli (Fedorenko et al., 2011; Pallier et al., 2011; Malik-Moraleda et al., 2022; Zaccarella et al., 2017). It has been proposed that the left vTPJ, lATL, inferior frontal gyrus (IFG),

and posterior superior temporal sulcus (pSTS) are the “classic high-level language-processing regions” (Fedorenko & Thompson-Schill, 2014) and together form the sentence-processing network (Dronkers et al., 2004; Labache et al., 2019; Matchin et al., 2019).

The traditional explanations for the roles of the left vTPJ and lATL in sentence processing are all based on the encoding and integration of general semantics and/or syntactic information (Humphries et al., 2006; Pallier et al., 2011; Price, 2010; Matchin et al., 2019). For example, Price (2010) reviewed 100 fMRI studies of speech comprehension and production and proposed that in sentence comprehension, the left lATL and angular gyrus (overlapping with the vTPJ) support amodal semantic combination and task-dependent semantic retrieval, respectively. In an influential fMRI study, Pallier et al. (2011) found that, in contrast to the left lFG and pSTS that responded even to abstract syntactic structures containing no content words, the left vTPJ and lATL only responded to meaningful sentences. They therefore proposed that the left vTPJ and lATL may bind syntactic roles to lexico-semantic representations to form high-level representations of semantic constituent structure. However, according to these general-semantic and/or syntactic accounts, it is difficult to understand why the same regions are especially sensitive to social semantics.

Here we propose a hypothesis that integrates the sentence and social-semantic sensitivity of the left vTPJ and lATL into one cognitive function, that is, social-semantic working memory. Our hypothesis is motivated by two existing views in literature. First, multiple brain regions ranging from sensory to association cortex can represent particular contents of working memory (Christophel et al., 2017; D’Esposito & Postle, 2015; Fuster, 1997; Postle, 2006). According to this view, the short-term retention of semantic information can be supported by the temporary activation of long-term memories (Cowan, 1998). Therefore, the left vTPJ and lATL that are assumed to support social concept representation can support social-semantic working memory. Second, sentences have more stable and durable semantic representation than fragmented linguistic stimuli, such as word lists. It has been found that when a series of words are presented very rapidly, recall is poor for word lists but near perfect for sentences (Potter et al., 1986; Potter, 1993). Based on this and related findings, Potter (1993; 2012) proposed that word meaning is activated rapidly, but the initial activation is highly unstable and will be forgotten within a few hundred milliseconds unless incorporated into a structure. Therefore, the sensitivity of brain regions to sentences may reflect either the semantic/syntactic integration itself or the semantic working memory consolidated by the semantic/syntactic integration. Given that most stimuli used in the previous studies of sentence processing are about people, the activation of the left vTPJ and lATL in these studies may reflect social-semantic working memory.

In this study, we examined the social-semantic-working-memory hypothesis using six fMRI experiments. First, we examined whether the sensitivity of the left vTPJ and lATL to sentences is selectively associated with social semantic comprehension (Experiments 1 and 2): the social-semantic-working-memory hypothesis predicts that the sensitivity of these regions to sentences could be found only if the sentences convey social meaning; the traditional general-semantic and/or syntactic accounts, however, predict that the sensitivity to sentences should be found even when the sentence conveys no social meaning. Second,

we examined a key prediction of the social-semantic-working-memory hypothesis that the left vTPJ and lATL should show persistent social-semantic-selective activity after the stimuli disappeared, i.e., demonstrating the key signature property of working memory (Experiments 3 and 4). Finally, we supplemented the above key examinations with two additional experiments, aiming to investigate whether the left vTPJ and lATL were involved in the processing of nonlinguistic, high-socialness stimuli (Experiment 5) and whether the left vTPJ and lATL had stronger intrinsic connectivity to the social-semantic-processing areas or to the sentence-processing areas (Experiment 6).

Results

Sentence sensitivity of the left vTPJ and lATL is selectively associated with social-semantic comprehension (Experiment 1 & 2)

The aim of Experiments 1 and 2 was to examine whether the sensitivity of the left vTPJ and lATL to sentences is selectively associated with social semantic comprehension. In both experiments, participants were asked to read the sentences and word lists during fMRI scanning. Following previous neuroimaging studies (Humphries et al., 2006; Labache et al., 2019; Pallier et al. 2011; Zaccarella et al., 2017), we subtracted the neural responses to word lists from those to sentences to reflect the sensitivity to sentences. For both sentence and word-list stimuli, we manipulated the socialness of their meanings, leading to four conditions, namely, the high-socialness-sentence (HSS), high-socialness-word-list (HSWL), nonsocial-sentence (NSS), and nonsocial-word-list (NSWL) conditions. In both experiments, the stimuli of the HSWL and NSWL conditions were constructed by pseudorandomly combining the constituent words of the HSS and NSS conditions, respectively (see Methods).

The major differences between Experiments 1 and 2 were the lengths and structures of the sentences. In Experiment 1, we used short sentences with the noun-verb-noun structure. Using this type of sentence has two advantages. First, syntactic complexity can be easily controlled by consistently using the noun-verb-noun structure in both sentence conditions. Second, because there are only content words, socialness can be manipulated word by word, which can maximize the social-semantic effect. Therefore, in Experiment 1, for the HSS condition, all constituent words of the sentences have high socialness (e.g., “ ”, meaning “(the) gangsters robbed (the) shops”); for the NSS condition, all constituent words of the sentences refer to natural and nonhuman entities and events (e.g., “ ”, meaning “(the) flood inundated (the) grassland”). See Fig. 1A and 1B for sample stimuli and trials.

Despite the advantages of using short sentences, natural sentences often consist of both content and function words and are often longer than three words. Therefore, we conducted Experiment 2 to examine whether the findings of Experiment 1 could be generalized to sentences with more natural structures and lengths. In Experiment 2, the sentences were approximately 8 words long for both conditions (see Table S15). The sentences of the HSS conditions were all related to interpersonal interactions or interpersonal relationships (e.g., “ ”, meaning “The head teacher should be responsible for managing the class order”), and the sentences of the NSS condition were all about natural and nonhuman entities and

events (“ ”, meaning “The long-term lack of water makes the shrubs here wither gradually”). See Fig. 2A and 2B for sample stimuli and trials.

The whole-brain results of Experiment 1 (Fig. 1C and Table S2) showed both social-semantic and sentence effects in the left vTPJ and lATL, replicating the findings of the literature (Zaccarela et al., 2017; Fedorenko et al., 2010; Lin et al., 2018a; Zhang et al., 2021). Importantly, significant interactions between social-semantic and sentence effects were found in both the left TPJ and lATL. We then examined the sentence effect using the high-socialness and nonsocial stimuli separately. The comparison between the HSS and HSWL conditions revealed significant sentence effects in the left vTPJ, lATL, and other canonical regions of the sentence-processing network; however, the comparison between the NSS and NSWL conditions did not reveal any significant sentence effect in either the left vTPJ or lATL. The whole-brain results of Experiment 2 replicated all of the main findings mentioned above, except that the significant interaction effect was found only in the left vTPJ (Fig. 2C and Table S3).

Because whole-brain analysis requires very rigorous corrections for multiple comparisons, its threshold is often too conservative to detect signal differences. Therefore, we further examined the results in the left vTPJ and lATL using ROI analysis. To reveal the robustness of the results, we used 2 different ways to define the ROIs: The first way was to define the ROIs based on a meta-analysis of the previous neuroimaging studies that compared sentences with word lists (Zaccarella et al., 2017); the second way was to define the ROIs based on the individual result of the sentence effect (“HSS + NSS” > “HSWL + NSWL”) on half of the data within predefined group-level masks of the left vTPJ and lATL (for details, see Methods). Because recent studies have found that the left vTPJ and lATL showed deactivation to the general task effort in ROI analysis (Kuhnke et al., 2022; Zhang et al., 2022), we regressed out the task-effort effect as reflected by the average inverse efficiency score (IES, which is defined as the mean reaction time divided by accuracy; Townsend & Ashby, 1983) of each condition and participant (see Methods). The ROI analyses found consistent patterns in the two experiments (see Fig. 1D, Fig. 2D, Table S7, and Table S8): In all ROIs, both Bayesian and classical parametric tests found an interaction between social-semantic and sentence effects, and simple effect analysis showed sentence effects only in the contrast between the high-socialness sentence and word list conditions (HSS > HSWL) but not in the contrast between the nonsocial sentence and word list conditions (NSS > NSWL).

In addition to these major results, we also examined the results using two supplementary baseline conditions of Experiment 1 that consist of high-socialness and nonsocial character lists and two supplementary individual ROIs located in the dorsal medial prefrontal cortex (dmPFC) and right vTPJ (where the sentence and social effects have also been reported by some previous studies). The result patterns using the supplementary baselines and ROIs were all similar to those of the major results (Figure S1, Figure S2, Table S1, Table S12, and Table S13).

Taken together, in both Experiments 1 and 2, we found the sentence sensitivity of the left vTPJ and lATL only when the sentences conveyed social meaning, which is robust to different sentence lengths and structures. This finding is consistent with the prediction of the social-semantic-working-memory

hypothesis but not that of the general-semantic and/or syntactic accounts for the neural activity of the left vTPJ and lATL.

Persistent social-semantic-selective neural activity in the left vTPJ and lATL (Experiment 3 & 4)

Working memory is characterized by persistent neural activity during the maintenance of information (Christophel et al., 2017; Sreenivasan & D'Esposito, 2019). Therefore, Experiments 3 and 4 examined whether the left vTPJ and lATL showed persistent social-semantic-selective neural activity after the linguistic stimuli that convey the social meanings disappeared.

Persistent social-semantic-selective neural activity during the delay period

In Experiment 3, we examined whether the left vTPJ and lATL showed persistent social-semantic-selective neural activity as reflected by the amplitude of the blood-oxygenation-level-dependent (BOLD) signals. Note that persistent neural activity is not always associated with the amplitude of BOLD signals; rather, in many cases, it reflects as multiple-voxel activation patterns (Postle, 2015). However, the social-semantic-working-memory hypothesis assumes that in the left vTPJ and lATL, the increase of BOLD signals in high-socialness sentence comprehension reflects social-semantic working memory. According to this assumption, similar effects should also be found during the maintenance of the sentences. To examine this prediction, participants accomplished a delayed recognition task during the fMRI scanning. Each trial contained three stages: in the encoding stage, participants read 2 or 4 sentences consisting of high-socialness or nonsocial words; in the maintenance stage, participants maintained the sentences for a period; and in the response stage, participants made responses to a force-choice word recognition task. The sentential stimuli were identical to those used in Experiment 1, each consisting of 3 words. See Fig. 3A and 3B for sample stimuli and trials.

We varied the number of sentences to manipulate the memory load. Memory load is a classic factor in working-memory studies and its effect has been reliably found in core fronto-parietal working-memory network (Manoach et al., 1997; Rottschy et al., 2012). In the brain regions that are assumed to selectively represent particular type of contents like objects, faces, and mental states, previous findings on load effects were inconsistent: some studies have found load effects for working memory of specific stimuli (Druzgal & D'Esposito, 2001; Meyer et al., 2015; Xu & Chun, 2006), but others have not (Martin et al., 2003; Song & Jiang, 2006; Thornton & Conway, 2013; Zhao et al., 2020). We therefore explored the interaction between social-semantic and load effects in the left vTPJ and lATL.

The whole-brain results of Experiment 3 are shown in Fig. 3C, Table S4, and Table S5. The left vTPJ and lATL showed the persistent social-semantic-selective activity predicted by the social-semantic-working-memory hypothesis: significant social-semantic effects (high-socialness > nonsocial), as reflected by the amplitude of the BOLD signals, were found in both regions at both the encoding and maintenance stages.

These regions, however, showed no significant response to the sentence number or interaction between the two factors at either the encoding or maintenance stages.

As in Experiments 1 and 2, we conducted ROI analyses to further examine the results within the left vTPJ and lATL. To remain consistent with Experiments 1 and 2, the ROIs were defined based on the results of Zaccarella et al. (2017). Unlike in Experiments 1 and 2, we were not able to define individual ROIs because Experiment 3 did not include any localizer; we also did not regress out the effect of task efforts because we explicitly manipulated the task demands (i.e. memory load) in this experiment.

The results of the ROI analysis are shown in Figure 3D and Table S9. Both Bayesian and classical parametric tests found social-semantic effects in both ROIs at both the encoding and maintenance stages, confirming the key prediction of the social-semantic-working-memory hypothesis. In addition, at the encoding stage, the social-semantic and sentence-number effects showed interactions in both ROIs: larger social-semantic effects were found in the 4-sentence conditions than in the 2-sentence conditions; however, no such effect was found at the maintenance stage. These findings indicate that the left vTPJ and lATL can show persistent social-semantic-selective neural activity; in addition, these regions are selectively sensitive to the encoding load of social-semantic information but insensitive to the maintenance load of it[1].

Persistent social-semantic-selective neural activity during the processing of successive sentences

Language comprehension often requires processing successive sentences, during which the meaning of the context sentences must be maintained while the current sentence is processed. In Experiment 4, we examined whether the left vTPJ and lATL showed persistent social-semantic-selective neural activity during the processing of successive sentences. We used multiple voxel pattern analyses (MVPA) to reveal the semantic contents of the neural representation, which allows decoding the maintained semantic representations of the context sentence from the neural activity associated with the presentation of the current sentence.

In Experiment 4, participants accomplished a novel ‘mental portrait’ task. In each trial, participants read two successive sentences describing two features of a person; then, they saw two photos of different people and decided which photo is more consistent with the preceding sentences by pressing buttons. In half of the trials, people read sentences about two trait dimensions, dominance and trustworthiness, which are the major trait dimensions associated with face evaluation (Oosterhof & Todorov, 2008). In the other half of the trials, people read sentences about two physical facial dimensions, which are the size of the face and the length of the eyebrows. Although the trait and physical facial dimensions are both person-related, the trait dimensions should have higher socialness than the physical ones because they are more directly related to interactions between people. To dissociate the brain activities associated with the presentation of the two sentences and the pictures, the sentences and pictures were separated by jitters (for task procedure, see Fig. 4A).

The key prediction of the experiment is that if the left vTPJ and lATL represent social-semantic working memory during the processing of successive sentences, then they should maintain the social meaning of the first sentence while the second sentence is being processed. Therefore, we performed MVPA to decode the poles of each dimension (e.g., high dominance vs. low dominance) expressed in the first sentence from the neural activity associated with the presentation of the second sentence. We also conducted MVPA to decode the poles of each dimension expressed in each sentence from the neural activity associated with the presentation of the sentence itself. The analyses were performed at both the whole-brain and ROI levels (see Methods). The whole-brain searchlight analysis failed to reveal any significant results. The ROI analysis was based on the same ROIs as in Experiment 3. As shown in Fig. 4C, in the left vTPJ, the poles of dominance expressed by the sentences could be decoded from both their concomitant and delayed neural activity (with average decoding accuracy of 3.22% and 6.05% above the 50% chance level and with p values of 0.010 and 0.001, respectively); in the left lATL, the poles of dominance expressed by the sentences could be decoded from their delayed neural activity (with average decoding accuracy of 3.52% above the 50% chance level and with a p value of 0.037), but the effect did not survive the Bonferroni correction for the number of dimensions decoded (N = 4). No other dimension could be decoded from either the concomitant or the delayed neural activity of the sentences. Therefore, our results partially confirmed the prediction of the social-semantic-working-memory hypothesis by showing that at least social-semantic information associated with dominance can be maintained in the left vTPJ (and possibly the lATL) during the processing of successive sentences.

Left vTPJ and lATL are sensitive to the socialness of nonlinguistic stimuli (Experiment 5)

The above experiments indicate that the neural activity of the left vTPJ and lATL during sentence processing is associated with social-semantic working memory rather than linguistic processes. However, because all of the above experiments used sentence stimuli to induce social-semantic processing, it was unclear whether the social-semantic sensitivity of the left vTPJ and lATL was specific to language comprehension.

In Experiment 5, we examined the sensitivity of the left vTPJ and lATL to the social information conveyed by nonlinguistic stimuli. Participants were asked to watch short silent videos and rate their pleasantness (for task procedures, see Fig. 5B). There were three kinds of videos corresponding to three conditions: The high-socialness videos were about interactions between people; the single-person videos contained only one person; and the nonsocial videos contained only natural and nonhuman entities.

The whole-brain results are shown in Fig. 5C and Table S6. In the left vTPJ, significant differences were found between each two of the three conditions, with the high-socialness condition evoking the strongest neural activity and the nonsocial condition evoking the weakest neural activity. The left lATL showed stronger activation to the high-socialness condition than to the nonsocial condition. A small cluster in the left dorsal ATL and temporal pole showed stronger activation to the single-person condition than to the nonsocial condition. Significant socialness effects were also found in many other brain regions of the

social-cognitive system (see Fig. 5C). The ROI results are shown in Fig. 5D and Table S10. The ROI analysis was based on the same ROIs used in Experiments 3 and 4. In both ROIs, both Bayesian and classical parametric tests found differences between each two of the three conditions, with the high-socialness condition evoking the strongest neural activity and the nonsocial condition evoking the weakest neural activity. Therefore, the left vTPJ and lATL are sensitive to social information, whether conveyed by linguistic or nonlinguistic stimuli.

Left vTPJ and lATL have stronger intrinsic connectivity to the social-semantic-processing areas than to the sentence-processing areas (Experiment 6)

According to the social-semantic-working-memory hypothesis, the function of the left vTPJ and lATL is intrinsically more tightly associated with social-semantic working memory than with linguistic processing. Therefore, these regions should have stronger intrinsic functional connectivity to the social-semantic-processing areas than to the sentence-processing areas. Experiment 6 examined this prediction using resting-state fMRI.

We defined the seed ROIs based on two previously published meta-analyses (key ROIs and sentence-processing ROIs: Zaccarella et al., 2017; social-semantic-processing ROIs: Zhang et al., 2021; see Fig. 6A). Both meta-analyses identified areas in the left vTPJ and lATL and the locations were very close to each other. To remain consistent with the ROI analyses of Experiments 1 to 5, we defined the key seed ROIs of the left vTPJ and lATL based on Zaccarella et al. (2017) and did not include the left vTPJ and lATL area identified by Zhang et al. (2021) as seed ROIs. According to our prediction, the left vTPJ and lATL should have stronger intrinsic connectivity to the social-semantic-processing areas than to the sentence-processing areas even they were defined based on sentence-processing tasks.

We first examined whether the left vTPJ and lATL have stronger resting-state functional connectivity (RSFC) to the remaining sentence-processing ROIs or to the social-semantic-processing ROIs. Both regions showed stronger RSFC to the social-semantic-processing ROIs than to the sentence-processing ones (Fig. 6B and Table S11). We then conducted a k-means cluster analysis based on the correlation matrix between all pairs of seed ROIs (see Methods). The silhouette score indicated that these nodes could be best grouped into 2 clusters (Fig. 6C). The results of the 2-cluster solution are shown in Fig. 6C. Four seed ROIs defined by the sentence-processing task, including the left vTPJ and lATL, and 2 ROIs close to the lATL, that is, the anterior superior temporal sulcus and temporal pole, clustered together with the social-semantic-processing ROIs, while the other sentence-processing ROIs clustered together. These results confirm our prediction that the left vTPJ and lATL have stronger intrinsic connectivity to the social-semantic-processing areas than to the sentence-processing areas.

[1] As mentioned above, previous findings were inconsistent in the load effects in the areas that are assumed to selectively represent particular type of contents. One possibility is that the emergence of such effects relies on task-dependent modulation by the core working-memory areas (Zhao et al., 2020). According to this view, at the maintenance stage, the lack of interaction effect in the left vTPJ and lATL

might be associated with the weakness of the load effect in the core fronto-parietal working-memory network as shown in Figure 3C.

Discussion

We examined the function of the left vTPJ and lATL in sentence processing and social-semantic working memory. Two key findings indicate that these regions engage in sentence processing through social-semantic working memory: First, they are more sensitive to sentences than to word lists only if the sentences convey social meaning (Experiments 1 and 2); second, they show persistent social-semantic-selective activity after the linguistic stimuli disappeared (Experiments 3 and 4). Two additional findings also indicate that these regions are more tightly associated with social-semantic processing than with linguistic processing: they are sensitive to the socialness of nonlinguistic stimuli (Experiment 5) and are intrinsically more tightly connected with the social-semantic-processing areas than with the sentence-processing areas (Experiment 6). Taken together, our results provide converging evidence for the social-semantic-working-memory hypothesis of the left vTPJ and lATL and challenge the general-semantic and/or syntactic accounts for the neural activity of these regions in sentence processing.

Our results indicate that during sentence processing, the stronger neural responses of the left vTPJ and lATL to sentences than to word lists are selectively associated with social-semantic comprehension, which is likely due to more durable working memory for coherent social meanings than for incoherent ones in these regions. It is notable that without controlling for the socialness of the stimuli, the activation of these regions in sentence processing has consistently been reported in the literature (Humphries et al., 2006; Pallier et al., 2011; Malik-Moraleda et al., 2022; Zaccarella et al., 2017). Why is the activity of the left vTPJ and lATL so frequently observed in previous studies of sentence processing? There are at least two reasons. First, language use is a social behavior so that sentences are naturally dominated by social semantic information (Olson et al., 2013). For example, it has been found that approximately 2/3 of natural conversations are of social topics (Dunbar et al., 1997). Second, the left vTPJ and lATL are sensitive to the social meaning of a very broad range of concepts (Zhang et al., 2022). For example, they are even sensitive to the social meaning of nonliving objects (Lin et al., 2019). Therefore, the comprehension of the vast majority of our daily language may require the involvement of social-semantic working memory.

Our results provide an alternative explanation for the results of previous neuroimaging studies that compare sentences with fragmented linguistic stimuli. The stronger brain activity to sentences than to nonsentential stimuli was viewed as a classic neural signature for linguistic processing. It has been used for localizing the language network (Fedorenko et al., 2010; 2011; Labache et al., 2019; Malik-Moraleda et al., 2022), examining the linguistic functions of the brain networks defined by resting-state fMRI data processing (Branco et al., 2020), and revealing the recruitment of the occipital cortex of congenitally blind individuals in linguistic processing (Bedny et al., 2011). However, our results show that, without controlling for the socialness of the stimuli, this classic effect may reflect social-semantic working memory. Therefore, the previous findings on this effect should be interpreted with caution, and future language studies should consider social-semantic processing in language comprehension.

Our results indicate that the left vTPJ and lATL may connect language comprehension with social cognition through social-semantic working memory. Most previous studies on the relationship between language and social cognition focused on the ability of reasoning about mental states, which is known as Theory of Mind (ToM; de Villiers, 2007; Ferstl et al., 2008; Hagoort, 2019; Lin et al., 2018b; Paunov et al., 2022). The key regions supporting ToM are the right TPJ and dorsal medial prefrontal cortex (Saxe & Wexler 2005; Schurz et al., 2014), which are often engaged in the comprehension of stories and nonliteral meanings (Feng et al., 2021; Ferstl et al., 2008; Mar, 2011). We assume that in comparison with ToM, social-semantic working memory is a more general and basic social-cognitive component that connects language comprehension with social cognition: it is not specific to mental states but involved in the processing of a wide range of social concepts; it forms the basis of social-semantic manipulation and integration, which in turn supports higher-order social cognition such as ToM. Consistent with our view, in the field of social neuroscience, the left vTPJ and lATL are associated with not only ToM (Lewis et al., 2011; Samson et al., 2004) but also other social functions (Olson et al., 2013; Saxe & Wexler 2005; Wang et al., 2017); in the field of language comprehension, the left vTPJ and lATL are involved in not only comprehension of stories (Mar, 2011) and nonliteral meanings (Rapp et al., 2012) but also social-semantic comprehension of sentences (Zhang et al., 2021), phrases (Lin et al., 2020; Yang & Bi, 2022), and words (Lin et al., 2015; 2018a; 2019; Wang et al., 2019).

As indicated by previous social neuroscience studies, the representation of social concepts relies on fine-grained social-semantic dimensions that have distinct neural correlates (Tamir et al., 2016; Thornton & Mitchell, 2018). In Experiment 4, we examined the social-semantic working memory of two specific trait dimensions, i.e. dominance and trustworthiness. Only dominance could be decoded from the neural activity of the left vTPJ and lATL. This finding is consistent with the previous finding that dominance is the most salient and conserved across the trait-state divide according to neural representation (Thornton & Mitchell, 2018). It also indicates that the left vTPJ and lATL may not represent all kinds of social-semantic dimensions. Many regions outside the left vTPJ and lATL have been found to represent specific social-semantic subdimensions (Hassabis et al., 2014; Van Overwalle et al., 2015; Tamir et al., 2016; Thornton & Mitchell, 2018). It remains to be investigated whether these regions support working memory on specific social-semantic subdimensions.

The left vTPJ and lATL showed very similar results in the current study, indicating that they share similar functions. Similar functional profiles of these two regions have also been revealed in previous studies of social-semantic processing (Zhang et al., 2022), language processing (Lerner et al., 2011; Pallier et al., 2011), and RSFC (Amft et al., 2014). Nevertheless, some functional differences between them have also been indicated by the literature. It has been found that the left lATL is more stably involved in word-level social-semantic processing (Zahn et al., 2007; Zhang et al., 2021), while the left vTPJ is more sensitive to discourse-level social-semantic processing (Lin et al., 2018b; Zhang et al., 2021). Therefore, the left lATL and vTPJ may play greater roles in social concept retrieval and integration, respectively. In addition, the left vTPJ also plays a role in cross-modal social-semantic integration: it is sensitive to both speeches and gestures that convey the communicative intents (Redcay et al., 2016) and is especially sensitive to co-speech gestures (Weisberg et al., 2017).

The finding that the left vTPJ is involved in social-semantic working memory can be linked to the previous finding that several functional subdivisions of the left TPJ support working-memory processes. In the field of language processing, the left supramarginal and angular gyri have been found to buffer phonological and semantic information, respectively (Martin et al. 2021; Yue et al., 2019; Yue & Martin, 2021). In the field of social cognition, Meyer and Collier (2020) found that the bilateral dorsal TPJ is involved in working memory of mental states of specific individuals such as characters from a television show. These findings, together with ours, indicate that the left TPJ as a whole may play important roles in working memory, with its different subdivisions supporting working memory of different types of information.

Finally, it should be noted that both the left TPJ and ATL contain multiple functional subdivisions that support different cognitive functions (Graves et al., 2022; Huth et al., 2016; Lin et al., 2018a; 2020; Seghier, 2013; Wang et al., 2019; Zhang et al., 2022). Hung et al. (2020) identified 4 functional subregions of the ATL using meta-analytic approaches. Among these subregions, only the lATL is sensitive to social processing; the other subregions are differently sensitive to linguistic processing, visual sensory, auditory sensory, episodic memory, and emotion (see also Wang et al., 2019). Lin et al. (2020) investigated the neural correlates of phrase-level semantic combination using phrases of high and low socialness. They found that in the left TPJ, the region sensitive to social semantics is ventral to the region sensitive to phrase-level general semantic combination, with no overlap between the two regions. Therefore, although we found that the activation of the left vTPJ and lATL in sentence processing is selectively associated with social-semantic comprehension, some other brain areas of the TPJ and ATL might be involved in general-semantic and/or syntactic processes.

To conclude, we examined whether the sentence and social-semantic effects observed in the left vTPJ and lATL both reflect social-semantic working memory. We found that the stronger responses of these regions to sentences than to word lists are selectively associated with social-semantic comprehension and that these regions are involved in social-semantic working memory during and after sentence processing, which supports the social-semantic-working-memory hypothesis. Our findings provide novel insights into the function of the left vTPJ and lATL in language comprehension and indicate that these regions may connect language with social cognition through social-semantic working memory.

Online Methods

Participants

Participants were all right-handed and native Chinese speakers. None of them had experienced psychiatric or neurological disorders or had sustained a head injury. The sample sizes of Experiments 1, 2, 3, 4, 5 and 6 were 20 (16 women, M age = 22.3 years, SD age = 2.3 years), 20 (13 women, M age = 23.5 years, SD age = 1.9 years), 20 (11 women, M age = 21.8 years, SD age = 2.4 years), 16 (9 women, M age = 24.0 years, SD age = 2.4 years), 20 (14 women, M age = 22.8 years, SD age = 2.7 years), and 39 (28 women, M age = 22.9 years, SD age = 2.2 years), respectively. There were 82 participants in total (56

women, M age = 22.7 years, SD age = 2.4 years). For Experiments 1 to 5, 70 participants took part in only 1 of the 5 experiments, 10 participants took part in 2 of them, and 2 participants took part in 3 of them. The participants of Experiment 6 were all from Experiments 1 and 2. Before the study began, all protocols and procedures were approved by the Institutional Review Board of the Magnetic Resonance Imaging Research Center of the Institute of Psychology of the Chinese Academy of Sciences. Each participant read and signed the informed consent form before taking part in the experiment.

Designs and procedures

Experiment 1

In addition to the 2 sentence conditions (HSS and NSS conditions) and 2 word-list conditions (HSWL and NSWL conditions) mentioned in the Results section, Experiment 1 also included 2 character-list conditions as another type of baseline. Because the contrast between sentences and word lists reveals the neural responses to sentence-level processing better than the contrast between sentences and character lists, we present and discuss the results of the latter contrast only in the Supplemental Information (Section A).

In the experiment, each of the 6 conditions contained 96 trials. For the HSS and NSS conditions, each trial consisted of two sentences. For both conditions, the stimuli consist of 96 different sentences, with each sentence being presented twice in different pairs. Five independent rating experiments (each recruiting 16 participants who did not participate in the fMRI experiment) were conducted to obtain the socialness, imageability, semantic familiarity, and semantic plausibility of the sentences and the socialness of the constituent words. The HSS and NSS conditions were significantly different in both word- and sentence-level socialness (HSS > NSS) and were matched on all the other ratings. The two conditions were also matched on log-transformed word frequency (Chinese Linguistic Data Consortium, 2003). See Table S14 of Supplemental Information Section B for the statistics of the manipulated and controlled variables of Experiment 1. We then segmented the sentences of the HSS and NSS conditions into words and characters. The constituent words and characters of the HSS condition were used to form the stimuli of the HSWL and high-socialness character-list (HSCL) conditions[2]; the constituent words and characters of the NSS condition were used to form the stimuli of the NSWL and nonsocial character-list (NSCL) conditions. Each trial of the word-list conditions consisted of six nouns or six verbs. Each trial of the character-list conditions consisted of 6 character pairs that did not form words.

The fMRI experiment included 6 runs of 9.9 minutes each, employing a block design. In the first and last 10 seconds of each run, participants were shown a fixation. Each run contained 4 blocks for each condition, with interblock intervals of 10 s. The order of blocks of different conditions was counterbalanced across runs and participants. Each block contained a cue and four trials, lasting 20 s in total. The cue was presented for one second, indicating whether the following stimuli were sentences, word lists, or character lists. The structure of a trial is shown in Fig. 1B. Words and character pairs were presented one by one for 500 milliseconds each. A fixation of 300 milliseconds appeared after the last word or character pair, followed by a probe word or character pair appearing for 1.35 s. As soon as the participants saw the probe word or character pair, they were asked to judge whether the probe stimulus

had been presented within the current trial quickly and accurately. Each trial ended with a fixation of 350 milliseconds.

Experiment 2

Experiment 2 included 2 sentence conditions (HSS and NSS conditions) and 2 word-list conditions (HSWL and NSWL conditions). The HSS and NSS conditions each contained 60 different sentences. Five independent rating experiments (each recruiting 16 participants who did not participate in the fMRI experiment) were conducted to obtain the socialness, imageability, semantic familiarity, semantic plausibility, and syntactic plausibility of the sentences. The HSS and NSS conditions were significantly different in the socialness of sentence meaning (HSS > NSS) and were matched on all the other ratings (Table S15). For each sentence, the maximum depth and mean depth of the syntactic nodes were calculated based on the bottom-up node tree obtained from the Chinese Stanford Parser (https://nlp.stanford.edu/software/lex-parser.shtml), serving as two measures of syntactic complexity. The HSS and NSS conditions were matched on both measures (Table S15). In addition, the HSS and NSS conditions were also matched on character number, word number, and mean log-transformed word frequency (Table S15. For both the HSS and NSS conditions, the 60 sentences were grouped into 15 blocks (each containing 4 sentences). The constituent words of each block were then shuffled and rearranged into 4 word lists to constitute the stimuli of the HSWL and NSWL conditions.

The fMRI experiment included 4 runs of 7.1 minutes each, employing a block design. In the first and last 10 seconds of each run, participants were shown a fixation. Each run contains 4 blocks for 3 conditions and 3 blocks for the other conditions, with interblock intervals of 10 s. The number and order of blocks for different conditions were counterbalanced across runs and participants. Each block contained a cue and four trials. The cue was presented for 1 second, indicating whether the following stimuli were sentences or word lists. The trial structure was the same as that of Experiment 1, except that each sentence or word list was presented for 4 seconds, with each constituent word within a trial having an equal length of presentation time (see Fig. 2B).

Experiment 3

Experiment 3 employed a delayed word-recognition task, in which participants were asked to read sentences, maintain them for a period, and then perform word-recognition judgment by pressing buttons. We manipulated the socialness and number of stimuli (2 or 4 sentences) to create four experimental conditions: the high-socialness and high-memory-load (HSHML), high-socialness and low-memory-load (HSLML), nonsocial and high-memory-load (NSHML), and nonsocial and low-memory-load (NSLML) conditions. Each condition contained 32 trials. The stimuli were the 96 high-socialness and 96 nonsocial sentences used in Experiment 1. Each sentence appeared in two different trials. As in Experiment 1, we matched the imageability, semantic familiarity, and semantic plausibility of the sentences and the log-transformed word frequency across conditions (Table S16).

The fMRI experiment included 4 runs of 12 minutes each, employing an event-related design. Each run included 32 trials, with 8 trials for each condition. The numbers and orders of the trials for different

conditions were counterbalanced across runs and participants. In the first and last 10 seconds of each run, participants were shown a fixation. In each trial, the encoding, maintenance, and recognition stages lasted 7, 6, and 3 seconds, respectively. The three stages were separated by two jitter intervals, each 0.5 to 2.5 seconds, with an average duration of 1.5 seconds (see Fig. 3B).

Experiment 4

Experiment 4 employed a novel 'mental portrait' task, in which participants read two sentences describing either two trait features of a person (dominance and trustworthiness) or two physical facial features (big/small face and long/short eyebrows) of a person successively and then chose a photograph from two to match the contents of the sentences. For the trait dimension of dominance, participants saw either the sentence "TA " (meaning "He or she likes to lead and command others") indicating high dominance or "TA " (meaning "He or she likes to follow and obey others") indicating low dominance. For the trait dimension of trustworthiness, participants saw either the sentence "TA " (meaning "He or she is a sincere and straightforward person") indicating high trustworthiness or "TA " (meaning "He or she is a smooth and changeable person") indicating low trustworthiness. For the two physical facial dimensions, participants saw "TA / " (meaning "He or she is a person with a big/small face") and "TA / " (meaning "He or she is a person with long/short eyebrows"). We chose the two physical facial dimensions based on the finding of Vernon et al. (2014) and the results of rating experiments on our stimuli (see below), both of which indicate that the correlations between dominance, trustworthiness and the two selected physical facial features were very low. Note that for each of four dimensions, the two sentences describing the different poles of the dimension were identical in syntactic structures, avoiding the confounding between the semantic and syntactic differences.

The different orders and contents of the sentences resulted in 8 trait and 8 physical facial conditions. The social conditions were labeled HDHT, HDLT, LDHT, LDLT, HTHD, HTLD, LTHD, and LTLD, in which the letters HD, LD, HT, and LT indicate high dominance, low dominance, high trustworthiness, and low trustworthiness, respectively. The physical facial conditions were labeled BFLE, BFSE, SFLE, SFSE, LEBF, LESF, SEBF, and SESF, in which BF, SF, LE, and SE indicate big face, small face, long eyebrow, and short eyebrow respectively. The picture stimuli were 128 photographs selected from the CAS-PEAL Chinese face database (Gao et al., 2008). Four rating experiments (each recruiting 16 participants who did not participate in the fMRI experiment) were conducted to rate each photograph on the two traits and two physical facial dimensions using 1–100 scales. The results showed that the correlations between the z-transformed scores of the photographs on any two of the four dimensions were low ($|r| < 0.15$). The photographs were then grouped into 64 pairs. Each pair of photographs was included in two trait conditions that were opposite in both trait dimensions (e.g., HDHT and LDLT) and two physical facial conditions that were opposite in both physical facial dimensions (e.g., BFLE and SFSE). Therefore, each condition contained 16 pairs of photographs, corresponding to 16 different trials of the condition.

The fMRI experiment included 8 runs of 436 seconds each, employing an event-related design. In the first and last 10 seconds of each run, participants were shown a fixation. Each run included 32 trials, with 2 trials for each condition. The orders of the trials of different conditions were counterbalanced across runs

and participants. The trial structure is shown in Fig. 4A. Each trial started with a red fixation of 0.2 seconds. Then, the first and second sentences appeared in turn, each lasting for 1.5 seconds, followed by a jitter fixation of 1.5 to 3.5 seconds (M = 2.5 seconds). The photographs were shown for 2 seconds, during which participants were asked to make their judgment by pressing buttons. Each trial ended with a jitter fixation of 1.3 to 4.3 seconds (M = 2.8 seconds).

Experiment 5

Experiment 5 included 3 conditions, each of which contained 30 short silent videos. The videos were obtained from online resources (https://www.videvo.net/free-stock-footage/). All videos were cut to 5 seconds long. We selected the stimuli of the three conditions based on the number of people shown in the video, with the HS videos containing multiple people who are interacting, the SP videos containing a single person, and the NS videos containing no person.

The fMRI experiment included a single run of 11 minutes 16 seconds, employing a block design. In the first and last 10 seconds of each run, participants were shown a fixation. There were 6 blocks for each condition. Each block contained 5 videos, each lasting 5 seconds, and 4 interstimulus fixations of 500 milliseconds (see Fig. 5B for the block structure). Participants were asked to rate their pleasantness while watching the video by pressing one of four number buttons (1 = very unpleased, 4 = very pleased).

Experiment 6

Experiment 6 collected resting-state fMRI data using a single run lasting 8 minutes. During the fMRI scanning, participants were asked to look at a white cross in the center of a black screen.

Image acquisition and preprocessing

Structural and functional data were collected using a GE Discovery MR750 3 T scanner at the Magnetic Resonance Imaging Research Center of the Institute of Psychology of the Chinese Academy of Sciences. For all experiments, T1-weighted structural images were obtained using a spoiled gradient-recalled pulse sequence in 176 sagittal slices with 1.0-mm isotropic voxels. From Experiments 1 to 5, functional BOLD data were collected using a gradient-echo echo-planar imaging sequence in 42 near-axial slices (repetition time = 2 seconds; echo time = 30 milliseconds; flip angle = 70°; matrix size = 64 × 64; voxel size = 3.0 mm × 3.0 mm × 3.0 mm). In Experiment 6, functional BOLD data were collected using a gradient-echo echo-planar imaging sequence in 33 axial slices (repetition time = 2 seconds, echo time = 30 milliseconds, flip angle = 90°, matrix size = 64 × 64; voxel size = 3.5 mm × 3.5 mm × 4.2 mm).

The fMRI data were preprocessed using the Statistical Parametric Mapping software (SPM12; http://www.fil.ion.ucl.ac.uk/spm/) and the advanced edition of DPARSF V4.3 (Yan & Zang, 2010) implemented in DPABI V3.0 (Yan et al., 2016). For the preprocessing of the task fMRI data, the first five volumes of each functional run were discarded to reach signal equilibrium. Slice timing and 3-D head motion correction were performed. Subsequently, a mean functional image was obtained for each participant, and the structural image of each participant was coregistered to the mean functional image. Thereafter, the structural image was segmented using a unified segmentation module (Ashburner &

Friston 2005). Next, a custom, study-specific template was generated by applying diffeomorphic anatomical registration through exponentiated lie algebra (DARTEL; Ashburner, 2007). The parameters obtained during segmentation were used to normalize the functional images of each participant into the Montreal Neurological Institute space by applying the deformation field estimated by segmentation. The functional images were subsequently spatially smoothed using a 6-mm full-width-half-maximum Gaussian kernel for univariate analysis but not for multivariate pattern analysis (MVPA).

For the preprocessing of the resting-state fMRI data, after the same procedure for univariate analysis, linear trends were removed to reduce the effects of low-frequency drifts. The effects of nuisance variables, including 24 rigid head motion parameters (Friston, Williams, Howard, Frackowiak, & Turner, 1996; Yan et al., 2013), white matter signal, and cerebrospinal fluid signal, were removed by linear regression from each voxel's time course. Temporal bandpass filtering (0.01–0.1 Hz) was performed to reduce the effects of high-frequency noises.

Data analysis

For the behavioral analyses and results of Experiments 1 to 5, please see the Supplemental Information (Section C). The fMRI data analyses were all conducted using SPM12 unless specifically stated.

Univariate analysis (Experiments 1, 2, 3, and 5)

First-level analysis

At the first level, general-linear-model (GLM) analyses were performed to explore the fixed effect of each regressor for each participant. In Experiments 1, 2, and 5, which used a block design, each condition was modeled as a regressor (Experiment 1: HSS, NSS, HSWL, NSWL, HSCL, and NSCL; Experiment 2: HSS, NSS, HSWL, and NSWL; Experiment 5: HS, SP, and NS), resulting in 6, 4, and 3 regressors, respectively. In Experiment 3, for each of the 4 conditions (HSHML, HSLML, NSHML, and NSLML), the 3 stages (encoding, maintenance, and recognition) and the jitter intervals before and after the maintenance stage were modeled as 4 regressors of interest, resulting in 16 regressors. The above regressors were modeled with boxcar waveforms convolved with the canonical hemodynamic response function (HRF). In addition, for each GLM, six head motion parameters obtained by head motion correction were included as nuisance regressors, and a high-pass filter (128 seconds) was used to remove low-frequency signal drift for each run.

Second-level analysis

The estimated beta-maps for each regressor obtained from the first-level analysis were entered into second-level (between-subject) random-effect analysis. For Experiments 1, 2, and 3, flexible factorial models were applied to accommodate their multifactor designs (Experiment 1: 2 x 3 within-subject design; Experiment 2: 2 x 2 within-subject design; Experiment 3: 2 x 2 within-subject design for each of the three trial stages). Contrasts of interest were examined using within-subject t-tests. For Experiments 1 and 2, the contrasts included “[(HSS + HSWL) - (NSS + NSWL)] / [(HSS + HSCL) - (NSS + NSCL)]” (the main effect

of socialness), “[(HSS + NSS) - (HSWL + NSWL)] / [(HSS + NSS) - (HSCL + NSCL)]” (the main effect of sentence sensitivity), “[(HSS - HSWL) - (NSS - NSWL)] / [(HSS - HSCL) - (NSS - NSCL)]” (the interaction of socialness and sentence sensitivity), and “(HSS - HSWL) / (NSS - NSWL) / (HSS - HSCL) / (NSS - NSCL)” (the sentence sensitivity effect in the high-socialness and nonsocial conditions). For experiment 3, at both the encoding and maintenance stages, the contrasts included “(HSHML + HSLML) - (NSHML + NSLML)” (the main effect of socialness), “(HSHML + NSHML) - (HSLML + NSLML)” (the main effect of cognitive demand), and “(HSHML - NSHML) - (HSLML - NSLML)” (the interaction of socialness and cognitive demand). For Experiment 5, after fitting the GLM, contrasts between each two of the three conditions were computed for every participant. The contrast images were then entered into one-sample t tests. For whole-brain analysis, multiple comparison corrections were conducted using cluster-level FWE correction ($p < .05$) as implemented in SPM12 (voxel-wise $p < .001$).

ROI analysis

For ROI analysis, we used two methods to define the left vTPJ and lATL areas sensitive to sentences. The first way was to define the ROIs based on a previously published meta-analysis (Zaccarella et al., 2017). Zaccarella et al. (2017) reported 11 peak MNI coordinates where sentences induced reliably stronger activity than word lists, among which we selected the coordinates of -44 -56 18 and – 54 – 4 -22 to represent the left vTPJ and lATL, respectively. We chose these coordinates because they are most consistent with the anatomical positions “vTPJ” and “lATL”. In addition, these coordinates are also very close to the peak coordinates reported by recently published meta-analyses on social semantic processing (Arioli et al., 2020; Zhang et al., 2021). For each coordinate, the ROI was defined as a 6-mm radius sphere centered on it.

The second way to define the ROIs was based on individual data. This method was applicable to Experiments 1 and 2 because the task used in these experiments can serve as a localizer for the brain areas sensitive to sentences. The localizing method was modified from the method proposed by Fedorenko et al. (2010). Fedorenko et al. (2010) provided a set of group-constrained masks for the areas involved in language processing (http://web.mit.edu/evlab/funcloc/). Because the masks covered broader regions than the left vTPJ and lATL, we overlapped the original group-constrained masks with a social-constrained map to obtain the neural overlaps between language and social cognition in the left vTPJ and lATL. The social-constrained map was defined by the Neurosynth meta-analysis (neurosynth.org; Yarkoni et al., 2011) using the term ‘social’ as the key word (association test; false discovery rate criterion of 0.01). We obtained 4 overlapping clusters larger than 100 voxels (voxel size = 3.0 mm × 3.0 mm × 3.0 mm), located in the left vTPJ, lATL, dmPFC, and right vTPJ (which are located within Fedorenko et al.’s group-constrained masks of the left posterior temporal lobe, left anterior temporal lobe, left superior frontal gyrus, and right middle-posterior temporal lobe, respectively). We therefore used these clusters as the group-constrained masks of this study, which were used to define the 2 major individual ROIs in the left vTPJ and lATL and 2 supplementary individual ROIs in the other 2 regions. For each participant, the data from the first half of scanning were used to define the individual ROIs. The group-constrained masks were intersected with the participant’s unthresholded t-maps of the

contrasts of “sentence > word-list” (i.e., HSS + NSS > HSWL + NSWL)[3]. For each participant, the 10% of voxels with the highest t-values in each mask were chosen as the individual ROI (Blank & Fedorenko, 2020). Then, the data from the second half of scanning were used to conduct the statistical analyses at the ROI level. We presented the results of the major ROIs in the main text and those of the supplementary ROIs in the Supplemental Information (Section A).

In ROI analysis, for each participant, the estimated beta-values for each regressor obtained from the GLM analysis were averaged across all voxels within each ROI. For Experiments 1 and 2, the influence of IES was regressed out from beta-values for each condition and subject. Specifically, for each ROI, a linear mixed model was fit to the participants’ beta value using the *lme4* package (Bates & Sarkar 2007) in *R* (R Core Team, 2020). This model included IES as the fixed effect and participant as a random factor with only a random intercept. The residuals were obtained and then entered into the contrast analysis. All contrasts of interest were identical to those of whole-brain analysis and were examined using both Bayesian and classical parametric t-tests in *R*. Bayesian tests were based on the *BayesFactor* package (Morey & Rouder, 2015), with a default Cauchy prior width of r = 0.707 for effect size on the alternative hypothesis (H1) (Rouder et al., 2012).

MVPA (Experiment 4)

First-level analysis

In Experiment 4, the first-level analysis contained two steps. The first step was GLM analysis. We built 8 regressors (corresponding to the 8 different sentences of our stimuli, see Fig. 4B) for the encoding stage of the first sentence, 16 regressors for the encoding stage of the second sentence (corresponding to the 16 sentence combinations, i.e. HDHT, HDLT, LDHT, LDLT, HTHD, HTLD, LTHD, LTLD, BFLE, BFSE, SFLE, SFSE, LEBF, LESF, SEBF, and SESF) and 16 regressors for the response stage. These regressors were all convolved with the canonical HRF. In addition, six head motion parameters were included as nuisance regressors, and a high-pass filter (128 seconds) was used to remove low-frequency signal drift for each run.

The second step was MVPA. We conducted both whole-brain searchlight MVPA and ROI-based MVPA. All classification procedures at both the whole-brain and ROI levels were implemented by the e1071 package (Meyer et al., 2019) and custom script in R (R Core Team, 2020). Whole-brain searchlight analysis was conducted within a group-based gray mask. To obtain the mask, the normalized structural image was segmented into different tissues for each participant. The resulting gray matter probabilistic images were resliced to the same spatial resolution as that of the functional image, averaged across participants, and thresholded at 0.25 to generate a binary mask for searchlight mapping. For each voxel within the gray matter mask, support vector machine (SVM) decoding was conducted within a 5 x 5 x 5 voxels cube centered at that voxel using the leave-one-run-out cross-validation approach (Cortes & Vapnik, 1995). For the encoding stages of both sentences, we trained 4 classifiers to discriminate the poles of the 4 dimensions (HD or LD, HT or LT, BF or SF, and LE or SE) described in the current sentence. For the encoding stages of the second sentence, we additionally trained 4 classifiers to discriminate the poles of

the 4 dimensions described in the context sentence (the first sentence). Before the SVM decoding was conducted, beta values within a cube were normalized to remove the common response pattern by subtracting the mean across the conditions to be discriminated. The resulting accuracy images were smoothed using a 6 mm FWHM Gaussian kernel for subsequent second-level statistical analyses.

ROI-based MVPA was conducted within the ROIs identical to those used in Experiment 3. After fitting the GLM, for each regressor of the encoding stage of the first and second sentences in each run, the estimated beta-values of all voxels within a given ROI mask were normalized and concatenated to form a fMRI pattern vector. Based on these fMRI pattern vectors, SVM decoding was conducted to discriminate the poles of the 4 dimensions described in the current or last sentences, just as in the whole-brain searchlight cubes.

Second-level analysis

For whole-brain searchlight MVPA, the second-level statistical analysis was conducted to examine whether the classification performance for each dimension within each cube was above the chance level using one-tailed one-sample t-tests. For ROI-level MVPA, the participant-wise bootstrapping method was conducted to obtain the statistical significance of the classification performance for each dimension. For each round of bootstrapping iteration, the dataset was resampled with replacement to create a pseudo sample keeping the original sample size, and the mean classification accuracy of the group was calculated. This procedure was repeated 5000 times to form a sampling distribution for each classification. The null distribution of each classification was generated by subtracting the veritable accuracy from the sampling distribution, and the veritable accuracy was then ranked against the null distribution to calculate the *p* value.

RSFC analyses (Experiment 6)

There were 15 seed ROIs in total, among which 2 key ROIs (i.e. the left vTPJ and lATL) and 9 sentence-processing ROIs were defined based on the meta-analysis results of Zaccarella et al. (2017) and 4 social-semantic-processing ROIs were defined based on the meta-analysis results of Zhang et al. (2021). For each pair of seed ROIs, each participant's mean time series of each seed ROI was calculated and correlated with each other. The correlation coefficients were then Fisher-transformed to represent the RSFC. We conducted two analyses to examine whether the left vTPJ and lATL have stronger RSFC to the social-semantic or sentence-processing areas. In the first analysis, for each key ROI, we compared its mean RSFC to the social-semantic-processing ROIs with that to the sentence-processing ROIs across participants using both Bayesian and classical parametric t-test. In the second analysis, the mean RSFC matrix of these 15 seed ROIs was transformed back to correlation coefficients and then applied with k-means clustering to group them into 2 to 10 clusters. The ideal number of clusters was selected on the basis of the highest silhouette score.

[2] Character pairs are often used as nonwords in the research of Chinese reading (e.g., Lin et al., 2016) so that we included the character-list conditions to serve as nonword baseline conditions. However, it should be noted that almost all Chinese characters have their own meanings. The meaning of a Chinese word is

often related with the meaning of its constituent characters. Therefore, the constituent characters of high-socialness words also have relatively high socialness in their meanings, so that we referred to the condition as the high-socialness character-list condition.

[3] For the supplemental analysis using character-list conditions as the baseline conditions, the ROIs were defined using the contrasts of “sentence > character-list” (i.e., HSS + NSS > HSCL + NSCL).

Declarations

Author Note

This research was supported by grants from the National Natural Science Foundation of China (31871105) to N.L., the Scientific Foundation of Institute of Psychology, Chinese Academy of Sciences (No. E2CX3625CX) to X.W. and N.L., and the National High-end Foreign Experts Recruitment Plan (Grant number G2022055007L) to X.W. The authors declare that they have no conflict of interest.
Correspondence should be addressed to Nan Lin (E-mail address: linn@psych.ac.cn), 16 Lincui Road, Key Laboratory of Behavioral Science, Institute of Psychology, Chinese Academy of Sciences, Beijing 100101, China.

Supplementary information

Supplemental Information includes the supplemental fMRI results (Section A), the statistics of the manipulated and controlled variables of Experiments 1, 2, and 3 (Section B), the behavior data analyses and the results of Experiments 1 to 5 (Section C).

Author contributions

G. Zhang and N. Lin conceived the study. G. Zhang, N. Lin, and W. Shi developed the methods. G. Zhang performed the investigation. G. Zhang performed the data analysis. N. Lin supervised the work. G. Zhang and N. Lin wrote the initial draft. All authors reviewed and edited the manuscript.

Competing interests

The authors declare no competing interests.

Acknowledge

This research was supported by grants from the National Natural Science Foundation of China (31871105) to N.L., the Scientific Foundation of Institute of Psychology, Chinese Academy of Sciences (No. E2CX3625CX) to X.W. and N.L., and the National High-end Foreign Experts Recruitment Plan (Grant number G2022055007L) to X.W.

References

1. Amft, M., Bzdok, D., Laird, A. R., Fox, P. T., Schilbach, L., & Eickhoff, S. B. (2015). Definition and characterization of an extended social-affective default network. Brain Structure & Function, *220*(2), 1031–1049.
2. Arioli, M., Gianelli, C., & Canessa, N. (2021). Neural representation of social concepts: a coordinate-based meta-analysis of fMRI studies. Brain Imaging & Behavior, *15*(4), 1912–1921.
3. Ashburner J. (2007). A fast diffeomorphic image registration algorithm. NeuroImage, *38*(1), 95–113.
4. Ashburner, J., & Friston, K. J. (2005). Unified segmentation. NeuroImage, *26*(3), 839–851.
5. Bates, D., Maechler, M., Bolker, B., Walker, S., Christensen, R.H.B., Singmann, H., Dai, B., Scheipl, F., Grothendieck, G., Green, P., Fox, J., Bauer, A., & Krivitsky., P.N. (2014). *lme4*: *Linear Mixed-Effects Models Using 'Eigen' and S4 Classes*. R package version 1.1–30. https://github.com/lme4/lme4/
6. Bedny, M., Pascual-Leone, A., Dodell-Feder, D., Fedorenko, E., & Saxe, R. (2011). Language processing in the occipital cortex of congenitally blind adults. *Proceedings of the National Academy of Sciences*, *108*(11), 4429–4434.
7. Binney, R. J., & Ramsey, R. (2020). Social Semantics: The role of conceptual knowledge and cognitive control in a neurobiological model of the social brain. Neuroscience & Biobehavioral Reviews, *112*, 28–38.
8. Blank, I. A., & Fedorenko, E. (2020). No evidence for differences among language regions in their temporal receptive windows. NeuroImage, *219*, 116925.
9. Branco, P., Seixas, D., & Castro, S. L. (2020). Mapping language with resting-state functional magnetic resonance imaging: A study on the functional profile of the language network. Human Brain Mapping, *41*(2), 545–560.
10. Bzdok, D., Hartwigsen, G., Reid, A., Laird, A. R., Fox, P. T., & Eickhoff, S. B. (2016). Left inferior parietal lobe engagement in social cognition and language. Neuroscience & Biobehavioral Reviews, *68*, 319–334.
11. Chinese Linguistic Data Consortium (2003). [Chinese lexicon] (CLDCLAC-2003-001) Beijing, China: Tsinghua University, State Key Laboratory of Intelligent Technology and Systems, and Chinese Academy of Sciences, Institute of Automation
12. Christophel, T. B., Klink, P. C., Spitzer, B., Roelfsema, P. R., & Haynes, J. D. (2017). The Distributed Nature of Working Memory. Trends in Cognitive Sciences, *21*(2), 111–124.
13. Contreras, J. M., Banaji, M. R., & Mitchell, J. P. (2012). Dissociable neural correlates of stereotypes and other forms of semantic knowledge. Social Cognitive & Affective Neuroscience, *7*(7), 764–770.
14. Cortes C, & Vapnik V. (1995). Support-vector networks. Machine Learning, *20*, 273–297.
15. Cowan, N. (1998). *Attention and memory: An integrated framework*. Oxford University Press.
16. de Villiers, J. (2007). The interface of language and theory of mind. Lingua, *117*(11), 1858–1878.
17. D'Esposito, M., & Postle, B. R. (2015). The cognitive neuroscience of working memory. Annual Review of Psychology, *66*, 115–142.

18. Diveica, V., Koldewyn, K., & Binney, R. J. (2021). Establishing a role of the semantic control network in social cognitive processing: A meta-analysis of functional neuroimaging studies. NeuroImage, *245*, 118702.
19. Dronkers, N. F., Wilkins, D. P., Van Valin Jr, R. D., Redfern, B. B., & Jaeger, J. J. (2004). Lesion analysis of the brain areas involved in language comprehension. Cognition, *92*(1–2), 145–177.
20. Druzgal, T. J., & D'Esposito, M. (2001). Activity in fusiform face area modulated as a function of working memory load. Cognitive Brain Research, 10(3), 355–364.
21. Dunbar, R. I. (2004). Gossip in evolutionary perspective. Review of General Psychology, *8*(2), 100–110.
22. Dunbar, R. I., Marriott, A., & Duncan, N. D. (1997). Human conversational behavior. Human Nature, *8*(3), 231–246.
23. Fedorenko, E., Behr, M. K., & Kanwisher, N. (2011). Functional specificity for high-level linguistic processing in the human brain. *Proceedings of the National Academy of Sciences*, *108*(39), 16428–16433.
24. Fedorenko, E., Hsieh, P. J., Nieto-Castañón, A., Whitfield-Gabrieli, S., & Kanwisher, N. (2010). New method for fMRI investigations of language: defining ROIs functionally in individual subjects. Journal of Neurophysiology, *104*(2), 1177–1194.
25. Fedorenko, E., & Thompson-Schill, S. L. (2014). Reworking the language network. Trends in Cognitive Sciences, *18*(3), 120–126.
26. Feng, W., Yu, H., & Zhou, X. (2021). Understanding particularized and generalized conversational implicatures: Is theory-of-mind necessary? Brain & Language, *212*, 104878.
27. Ferstl, E. C., Neumann, J., Bogler, C., & Von Cramon, D. Y. (2008). The extended language network: a meta-analysis of neuroimaging studies on text comprehension. Human Brain Mapping, *29*(5), 581–593.
28. Friston, K. J., Williams, S., Howard, R., Frackowiak, R. S., & Turner, R. (1996). Movement-related effects in fMRI time-series. Magnetic Resonance in Medicine, *35*(3), 346–355.
29. Fuster J. M. (1997). Network memory. Trends in Neurosciences, *20*(10), 451–459.
30. Gao, W., Cao, B., Shan, S., Chen, X., Zhou, D., Zhang, X., & Zhao, D. (2008). The CAS-PEAL large-scale chinese face database and baseline evaluations. IEEE Transactions on Systems, Man, and Cybernetics - Part A: Systems and Humans, 38(1), 149–161.
31. Graves, W. W., Purcell, J., Rothlein, D., Bolger, D. J., Rosenberg-Lee, M., & Staples, R. (2022). Correspondence between cognitive and neural representations for phonology, orthography, and semantics in supramarginal compared to angular gyrus. Brain Structure & Function. https://doi.org/10.1007/s00429-022-02590-y
32. Hagoort, P. (2019). The neurobiology of language beyond single-word processing. Science, *366*(6461), 55–58.
33. Hassabis, D., Spreng, R. N., Rusu, A. A., Robbins, C. A., Mar, R. A., & Schacter, D. L. (2014). Imagine all the people: how the brain creates and uses personality models to predict behavior. Cerebral Cortex,

24(8), 1979–1987.

34. Humphries, C., Binder, J. R., Medler, D. A., & Liebenthal, E. (2006). Syntactic and semantic modulation of neural activity during auditory sentence comprehension. Journal of Cognitive Neuroscience, *18*(4), 665–679.
35. Hung, J., Wang, X., Wang, X., & Bi, Y. (2020). Functional subdivisions in the anterior temporal lobes: a large scale meta-analytic investigation. Neuroscience & Biobehavioral Reviews, *115*, 134–145.
36. Huth, A. G., De Heer, W. A., Griffiths, T. L., Theunissen, F. E., & Gallant, J. L. (2016). Natural speech reveals the semantic maps that tile human cerebral cortex. Nature, *532*(7600), 453–458.
37. Kuhnke, P., Chapman, C. A., Cheung, V. K. M., Turker, S., Graessner, A., Martin, S., Williams, K. A., & Hartwigsen, G. (2022). The role of the angular gyrus in semantic cognition: a synthesis of five functional neuroimaging studies. Brain Structure & Function, 10.1007/s00429-022-02493-y.
38. Labache, L., Joliot, M., Saracco, J., Jobard, G., Hesling, I., Zago, L., Mellet, E., Petit, L., Crivello, F., Mazoyer, B., & Tzourio-Mazoyer, N. (2019). A SENtence Supramodal Areas AtlaS (SENSAAS) based on multiple task-induced activation mapping and graph analysis of intrinsic connectivity in 144 healthy right-handers. Brain Structure & Function, *224*(2), 859–882.
39. Lerner, Y., Honey, C. J., Silbert, L. J., & Hasson, U. (2011). Topographic mapping of a hierarchy of temporal receptive windows using a narrated story. Journal of Neuroscience, *31*(8), 2906–2915.
40. Lewis, P. A., Rezaie, R., Brown, R., Roberts, N., & Dunbar, R. I. (2011). Ventromedial prefrontal volume predicts understanding of others and social network size. NeuroImage, *57*(4), 1624–1629.
41. Lin, N., Bi, Y., Zhao, Y., Luo, C., & Li, X. (2015). The theory-of-mind network in support of action verb comprehension: evidence from an fMRI study. Brain & Language, *141*, 1–10.
42. Lin, N., Wang, X., Xu, Y., Wang, X., Hua, H., Zhao, Y., & Li, X. (2018a). Fine subdivisions of the semantic network supporting social and sensory–motor semantic processing. Cerebral Cortex, *28*(8), 2699–2710.
43. Lin, N., Xu, Y., Wang, X., Yang, H., Du, M., Hua, H., & Li, X. (2019). Coin, telephone, and handcuffs: Neural correlates of social knowledge of inanimate objects. Neuropsychologia, *133*, 107187.
44. Lin, N., Xu, Y., Yang, H., Zhang, G., Zhang, M., Wang, S., … Li, X. (2020). Dissociating the neural correlates of the sociality and plausibility effects in simple conceptual combination. Brain Structure & Function, *225*(3), 995–1008.
45. Lin, N., Yang, X., Li, J., Wang, S., Hua, H., Ma, Y., & Li, X. (2018b). Neural correlates of three cognitive processes involved in theory of mind and discourse comprehension. Cognitive, Affective, & Behavioral Neuroscience, *18*(2), 273–283.
46. Lin, N., Yu, X., Zhao, Y., & Zhang, M. (2016). Functional Anatomy of Recognition of Chinese Multi-Character Words: Convergent Evidence from Effects of Transposable Nonwords, Lexicality, and Word Frequency. PloS one, *11*(2), e0149583.
47. Malik-Moraleda, S., Ayyash, D., Gallée, J., Affourtit, J., Hoffmann, M., Mineroff, Z., Jouravlev, O., & Fedorenko, E. (2022). An investigation across 45 languages and 12 language families reveals a

universal language network. Nature Neuroscience, *25*(8), 1014–1019. https://doi.org/10.1038/s41593-022-01114-5

48. Manoach, D. S., Schlaug, G., Siewert, B., Darby, D. G., Bly, B. M., Benfield, A., … Warach, S. (1997). Prefrontal cortex fMRI signal changes are correlated with working memory load. Neuroreport, 8(2), 545–549.
49. Mar, R. A. (2011). The neural bases of social cognition and story comprehension. Annual Review of Psychology, *62*(1), 103–134.
50. Martin, R. C., Ding, J., Hamilton, A. C., & Schnur, T. T. (2021). Working memory capacities neurally dissociate: evidence from acute stroke. Cerebral Cortex Communications, *2*(2), tgab005.
51. Martin, R. C., Wu, D., Freedman, M., Jackson, E. F., & Lesch, M. (2003). An event-related fmri investigation of phonological versus semantic short-term memory. Journal of Neurolinguistics, *16*, 341–360.
52. Matchin, W., Brodbeck, C., Hammerly, C., & Lau, E. (2019). The temporal dynamics of structure and content in sentence comprehension: Evidence from fMRI-constrained MEG. Human Brain Mapping, *40*(2), 663–678.
53. Meyer, D., Dimitriadou, E., Hornik, K., Weingessel, A., Leisch, F., Chang, C. C., & Meyer, M. D. (2019). Package “e1071”. The R Journal.
54. Mellem, M. S., Jasmin, K. M., Peng, C., & Martin, A. (2016). Sentence processing in anterior superior temporal cortex shows a social-emotional bias. Neuropsychologia, *89*, 217–224.
55. Meyer, M. L., & Collier, E. (2020). Theory of mind s: managing mental state inferences in working memory is associated with the dorsomedial subsystem of the default network and social integration. Social Cognitive and Affective Neuroscience, *15*(1), 63–73.
56. Meyer, M. L., Taylor, S. E., & Lieberman, M. D. (2015). Social working memory and its distinctive link to social cognitive ability: an fMRI study. Social Cognitive & Affective Neuroscience, *10*(10), 1338–1347.
57. Morey, R. D., & Rouder, J. N. (2015). *BayesFactor 0.9.12–4.3*. Comprehensive R Archive Network. https://richarddmorey.github.io/BayesFactor/
58. Olson, I. R., McCoy, D., Klobusicky, E., & Ross, L. A. (2013). Social cognition and the anterior temporal lobes: a review and theoretical framework. Social Cognitive & Affective Neuroscience, *8*(2), 123–133.
59. Oosterhof, N. N., & Todorov, A. (2008). The functional basis of face evaluation. *Proceedings of the National Academy of Sciences*, *105*(32), 11087–11092.
60. Pallier, C., Devauchelle, A. D., & Dehaene, S. (2011). Cortical representation of the constituent structure of sentences. *Proceedings of the National Academy of Sciences*, *108*(6), 2522–2527.
61. Paunov, A., Blank, I., Jouravlev, O., Mineroff, Z., Gallée, J., & Fedorenko, E. (2022). Differential tracking of linguistic vs. mental state content in naturalistic stimuli by language and Theory of Mind (ToM) brain networks. Neurobiology of Language, *3*(3), 413–440.
62. Pexman, P. M., Diveica, V., & Binney, R. J. (2022). Social Semantics: The Organisation and Grounding of Abstract Concepts. Philosophical Transactions of The Royal Society B: Biological Sciences, *378*,

20210363.

63. Postle B. R. (2006). Working memory as an emergent property of the mind and brain. Neuroscience, *139*(1), 23–38.
64. Postle B. R. (2015). The cognitive neuroscience of visual short-term memory. Current Opinion in Behavioral Sciences, *1*, 40–46.
65. Potter, M. C. (1993) Very short-term conceptual memory. Memory & Cognition, *21*, 156–161.
66. Potter, M. C. (2012). Conceptual short term memory in perception and thought. Frontiers in Psychology, *3*, 113.
67. Potter, M. C., Kroll, J. F., Yachzel, B., Carpenter, E., & Sherman, J. (1986). Pictures in sentences: understanding without words. Journal of Experimental Psychology: General, *115*(3), 281–294.
68. Price C. J. (2010). The anatomy of language: a review of 100 fMRI studies published in 2009. Annals of the New York Academy of Sciences, *1191*, 62–88.
69. R Core Team. (2020). *R: A language and environment for statistical computing* (Version 4.0.0) [Computer software]. Retrieved from https://cran.r-project.org. (R packages retrieved from MRAN snapshot 2020-08-24).
70. Rapp, A. M., Mutschler, D. E., & Erb, M. (2012). Where in the brain is nonliteral language? A coordinate-based meta-analysis of functional magnetic resonance imaging studies. NeuroImage, *63*(1), 600–610.
71. Redcay, E., Velnoskey, K. R., & Rowe, M. L. (2016). Perceived communicative intent in gesture and language modulates the superior temporal sulcus. Human Brain Mapping, *37*(10), 3444–3461.
72. Richardson, H., Koster-Hale, J., Caselli, N., Magid, R., Benedict, R., Olson, H., … Saxe, R. (2020). Reduced neural selectivity for mental states in deaf children with delayed exposure to sign language. Nature Communications, *11*(1), 1–13.
73. Rottschy, C., Langner, R., Dogan, I., Reetz, K., Laird, A. R., Schulz, J. B., Fox, P. T., & Eickhoff, S. B. (2012). Modelling neural correlates of working memory: a coordinate-based meta-analysis. NeuroImage, *60*(1), 830–846.
74. Rouder, J. N., Morey, R. D., Speckman, P. L., & Province, J. M. (2012). Default Bayes factors for ANOVA designs. Journal of Mathematical Psychology, *56*(5), 356–374.
75. Samson, D., Apperly, I. A., Chiavarino, C., & Humphreys, G. W. (2004). Left temporoparietal junction is necessary for representing someone else's belief. Nature Neuroscience, *7*(5), 499–500.
76. Saxe, R., & Wexler, A. (2005). Making sense of another mind: the role of the right temporo-parietal junction. Neuropsychologia, *43*(10), 1391–1399.
77. Schurz, M., Radua, J., Aichhorn, M., Richlan, F., & Perner, J. (2014). Fractionating theory of mind: a meta-analysis of functional brain imaging studies. Neuroscience & Biobehavioral Reviews, *42*, 9–34.
78. Schurz, M., Radua, J., Tholen, M. G., Maliske, L., Margulies, D. S., Mars, R. B., … Kanske, P. (2021). Toward a hierarchical model of social cognition: A neuroimaging meta-analysis and integrative review of empathy and theory of mind. Psychological Bulletin, *147*(3), 293.

79. Scott, S. K. (2019). From speech and talkers to the social world: The neural processing of human spoken language. Science, *366*(6461), 58–62.
80. Seghier, M. L. (2013). The angular gyrus: multiple functions and multiple subdivisions. The Neuroscientist, *19*(1), 43–61.
81. Song, J. H., & Jiang, Y. (2006). Visual working memory for simple and complex features: an fMRI study. NeuroImage, *30*(3), 963–972.
82. Spunt, R. P., Kemmerer, D., & Adolphs, R. (2016). The neural basis of conceptualizing the same action at different levels of abstraction. Social Cognitive & Affective Neuroscience, *11*(7), 1141–1151.
83. Sreenivasan, K. K., & D'Esposito, M. (2019). The what, where and how of delay activity. Nature reviews. Neuroscience, *20*(8), 466–481.
84. Tamir, D. I., Thornton, M. A., Contreras, J. M., & Mitchell, J. P. (2016). Neural evidence that three dimensions organize mental state representation: Rationality, social impact, and valence. *Proceedings of the National Academy of Sciences*, *113*(1), 194–199.
85. Thornton, M. A., & Conway, A. R. (2013). Working memory for social information: chunking or domain-specific buffer?. NeuroImage, *70*, 233–239.
86. Thornton, M. A., & Mitchell, J. P. (2018). Theories of person perception predict patterns of neural activity during mentalizing. Cerebral Cortex, *28*(10), 3505–3520.
87. Townsend, J.T., & Ashby, F.G. (1983). *Stochastic modeling of elementary psychological processes*. Cambridge: Cambridge University Press.
88. Van Overwalle, F., Ma, N., & Baetens, K. (2016). Nice or nerdy? The neural representation of social and competence traits. Social Neuroscience, *11*(6), 567–578.
89. Vernon, R. J., Sutherland, C. A., Young, A. W., & Hartley, T. (2014). Modeling first impressions from highly variable facial images. Proceedings of the National Academy of Sciences of the United States of America, *111*(32), E3353–E3361.
90. Wang, X., Wang, B., & Bi, Y. (2019). Close yet independent: Dissociation of social from valence and abstract semantic dimensions in the left anterior temporal lobe. Human Brain Mapping, *40*(16), 4759–4776.
91. Wang, Y., Collins, J. A., Koski, J., Nugiel, T., Metoki, A., & Olson, I. R. (2017). Dynamic neural architecture for social knowledge retrieval. *Proceedings of the National Academy of Sciences*, *114*(16), E3305–E3314.
92. Weisberg, J., Hubbard, A. L., & Emmorey, K. (2017). Multimodal integration of spontaneously produced representational co-speech gestures: an fMRI study. Language, Cognition & Neuroscience, *32*(2), 158–174.
93. Xu, Y., & Chun, M. M. (2006). Dissociable neural mechanisms supporting visual short-term memory for objects. Nature, *440*(7080), 91–95.
94. Yan, C. G., Cheung, B., Kelly, C., Colcombe, S., Craddock, R. C., Di Martino, A., Li, Q., Zuo, X. N., Castellanos, F. X., & Milham, M. P. (2013). A comprehensive assessment of regional variation in the impact of head micromovements on functional connectomics. NeuroImage, *76*, 183–201.

95. Yan, C. G., Wang, X. D., Zuo, X. N., & Zang, Y. F. (2016). DPABI: Data Processing & Analysis for (Resting-State) Brain Imaging. Neuroinformatics, 14(3), 339–351.
96. Yan, C.G., & Zang, Y. (2010). DPARSF: A MATLAB Toolbox for "Pipeline" Data Analysis of Resting-State fMRI. Frontiers in Systems Neuroscience, *4*, 13.
97. Yang, H., & Bi, Y. (2022). From words to phrases: neural basis of social event semantic composition. Brain Structure & Function, *227*(5), 1683–1695.
98. Yarkoni, T., Poldrack, R. A., Nichols, T. E., Van Essen, D. C., & Wager, T. D. (2011). Large-scale automated synthesis of human functional neuroimaging data. Nature Methods, *8*(8), 665–670.
99. Yue, Q., & Martin, R. C. (2021). Maintaining verbal short-term memory representations in non-perceptual parietal regions. Cortex, *138*, 72–89.
100. Yue, Q., Martin, R. C., Hamilton, A. C., & Rose, N. S. (2019). Non-perceptual Regions in the Left Inferior Parietal Lobe Support Phonological Short-term Memory: Evidence for a Buffer Account?. Cerebral Cortex, *29*(4), 1398–1413.
101. Zaccarella, E., Schell, M., & Friederici, A. D. (2017). Reviewing the functional basis of the syntactic Merge mechanism for language: A coordinate-based activation likelihood estimation meta-analysis. Neuroscience & Biobehavioral Reviews, *80*, 646–656.
102. Zahn, R., Moll, J., Krueger, F., Huey, E. D., Garrido, G., & Grafman, J. (2007). Social concepts are represented in the superior anterior temporal cortex. *Proceedings of the National Academy of Sciences*, *104*(15), 6430–6435.
103. Zhang, G., Hung, J., & Lin, N. (2022). Coexistence of the social semantic effect and non-semantic effect in the default mode network. Brain Structure & Function, 1–19.
104. Zhang, G., Xu, Y., Zhang, M., Wang, S., & Lin, N. (2021). The brain network in support of social semantic accumulation. Social Cognitive & Affective Neuroscience, *16*(4), 393–405.
105. Zhao, Y., Kuai, S., Zanto, T. P., & Ku, Y. (2020). Neural Correlates Underlying the Precision of Visual Working Memory. Neuroscience, *425*, 301–311.

Figures

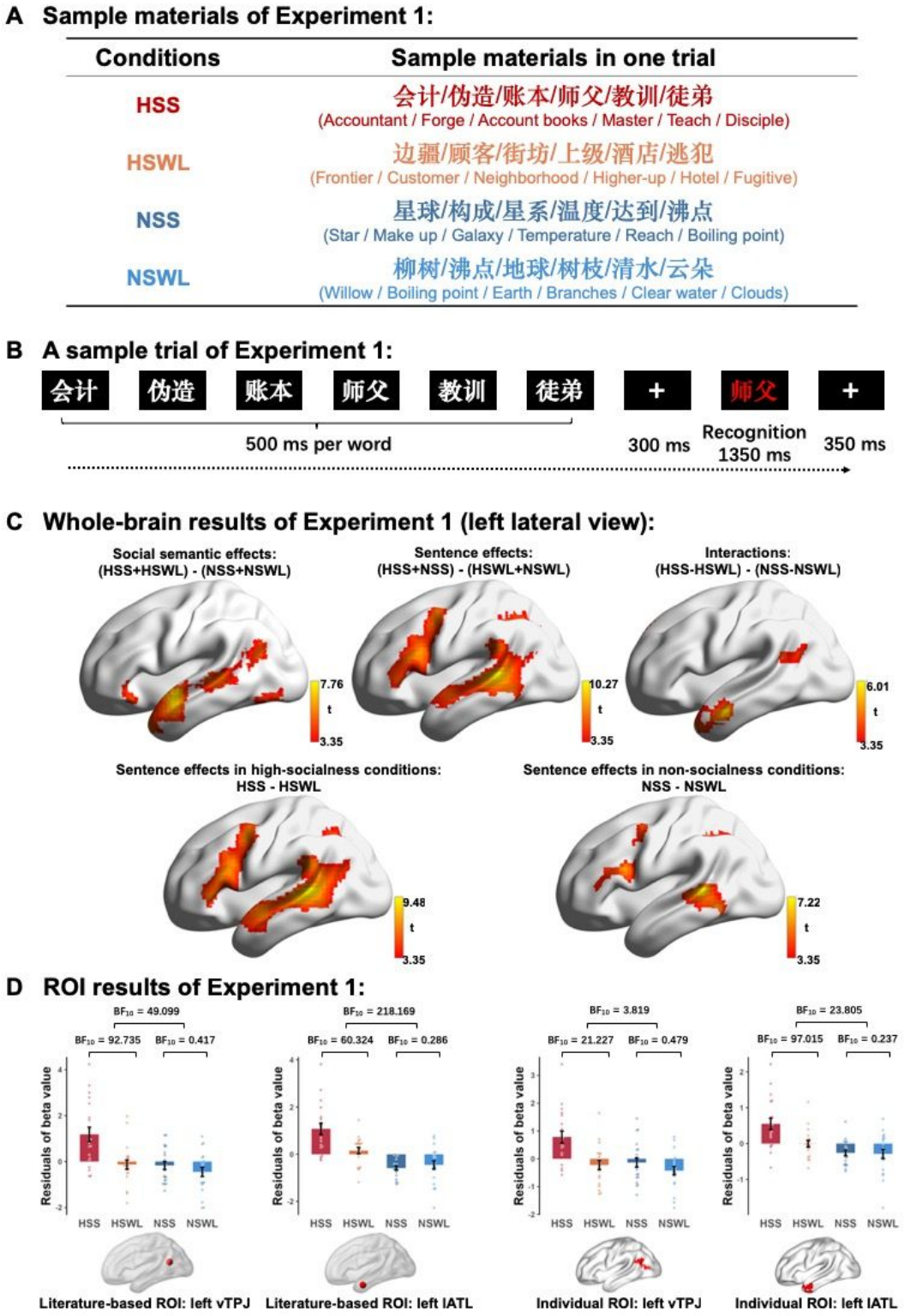

Figure 1

Sensitivity of the left vTPJ and lATL to sentences are selectively associated with social-semantic comprehension (Experiment 1).

Panel A: The sample materials for each critical experimental condition. For each trial, the stimuli were six words of either high or no socialness. The words formed two short sentences or an unconnected word list.

Slashes indicate the word boundaries.

Panel B: The trial structure of the task. In each trial, participants saw the stimuli word by word and then performed a word recognition task. The experiment used a block design, with each block consisting of four trials of the same condition.

Panel C: The left lateral view of the whole-brain results (for the full results, see Table S2). Interaction between social-semantic and sentence effects was found in the left vTPJ and lATL. The left vTPJ and lATL showed stronger activation to sentences than to word lists in the high-socialness conditions (HSS vs. HSWL) but not in the nonsocial conditions (NSS vs. NSWL).

Panel D: The ROI results (for the results of classical parametric tests, see Table S7). The two bar graphs on the left side show the results in the ROIs defined based on a meta-analysis for the contrast between sentences and word lists (Zaccarella et al., 2017). The two bar graphs on the right side show the results in the ROIs defined based on the contrast between sentences and word lists on half of individual data. The bars show the mean residuals of the beta values with the IES being regressed out, the errorbars show standard errors, and each point shows the data of a participant. The brain maps at the bottom of the bar graphs show the locations of the literature-based ROIs and the group-constrained masks for individual ROIs. All ROIs show strong sentence effect in high-socialness conditions, no sentence effect in nonsocial conditions, and interaction between social-semantic and sentence effects.

Abbreviations: HSS = high-socialness sentence, HSWL = high-socialness word list, NSS = nonsocial sentence, NSWL = nonsocial word list.

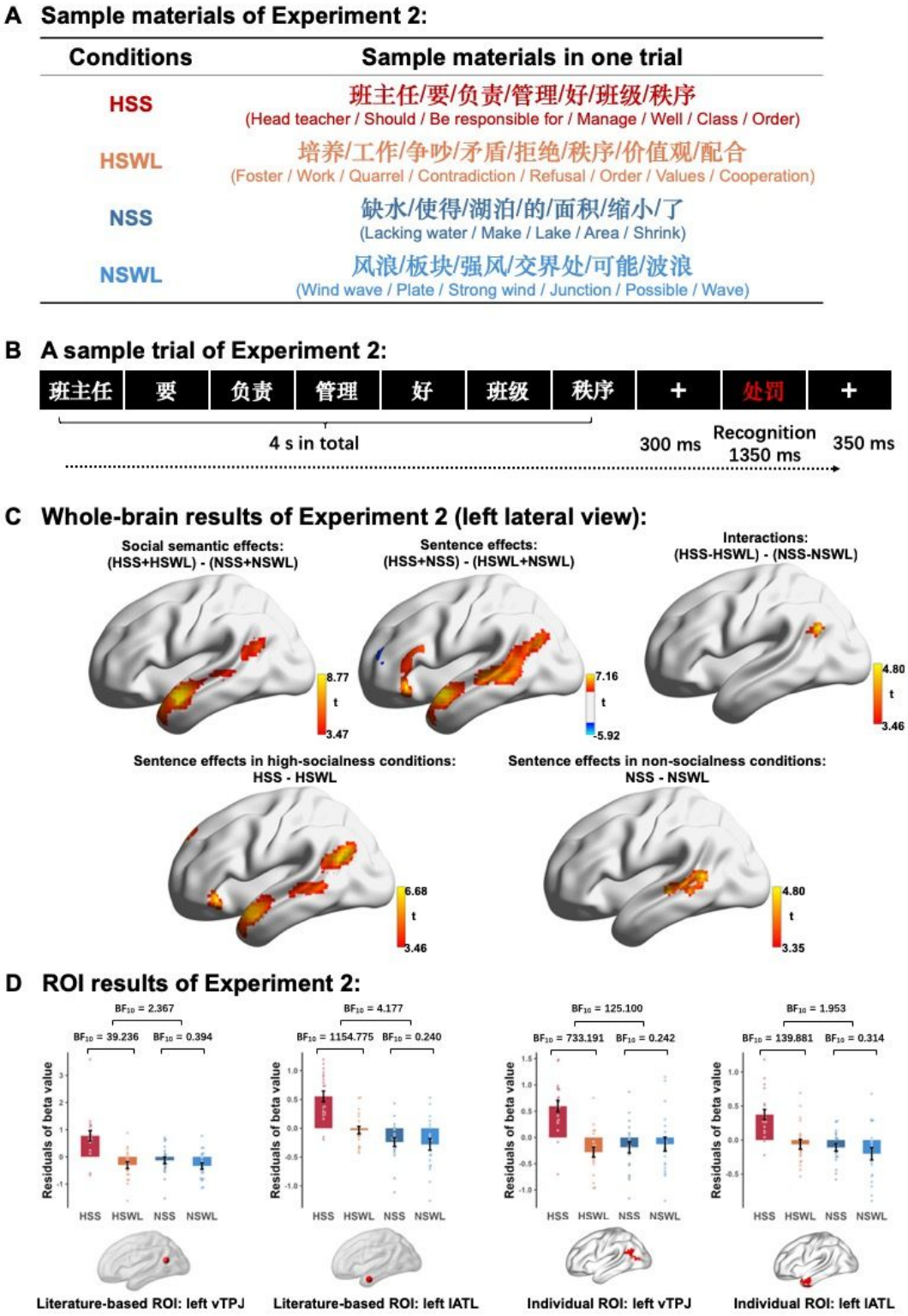

Figure 2

Replicating the finding of Experiment 1 using longer and more natural sentential stimuli (Experiment 2).

Panel A: The sample materials for each experimental condition. For each trial, the stimuli were a series of words that formed either a sentence or a word list of either high or no socialness. Slashes indicate the word boundaries.

Panel B: The trial structure of the task. The task was the same as that used in Experiment 1.

Panel C: The left lateral view of the whole-brain results (for the full results, see Table S3). Interaction between social-semantic and sentence effects was found in the left vTPJ. As in Experiment 1, the left vTPJ and lATL showed stronger activation to sentences than to word lists in the high-socialness conditions (HSS vs. HSWL) but not in the nonsocial conditions (NSS vs. NSWL).

Panel D: The ROI results (for the results of classical parametric tests, see Table S8). The layouts are identical to those of Figure 1D. The results replicate the finding of Figure 1D: All ROIs show strong sentence effect in high-socialness conditions, no sentence effect in nonsocial conditions, and interaction between social-semantic and sentence effects.

Abbreviations: HSS = high-socialness sentence, HSWL = high-socialness word list, NSS = nonsocial sentence, NSWL = nonsocial word list.

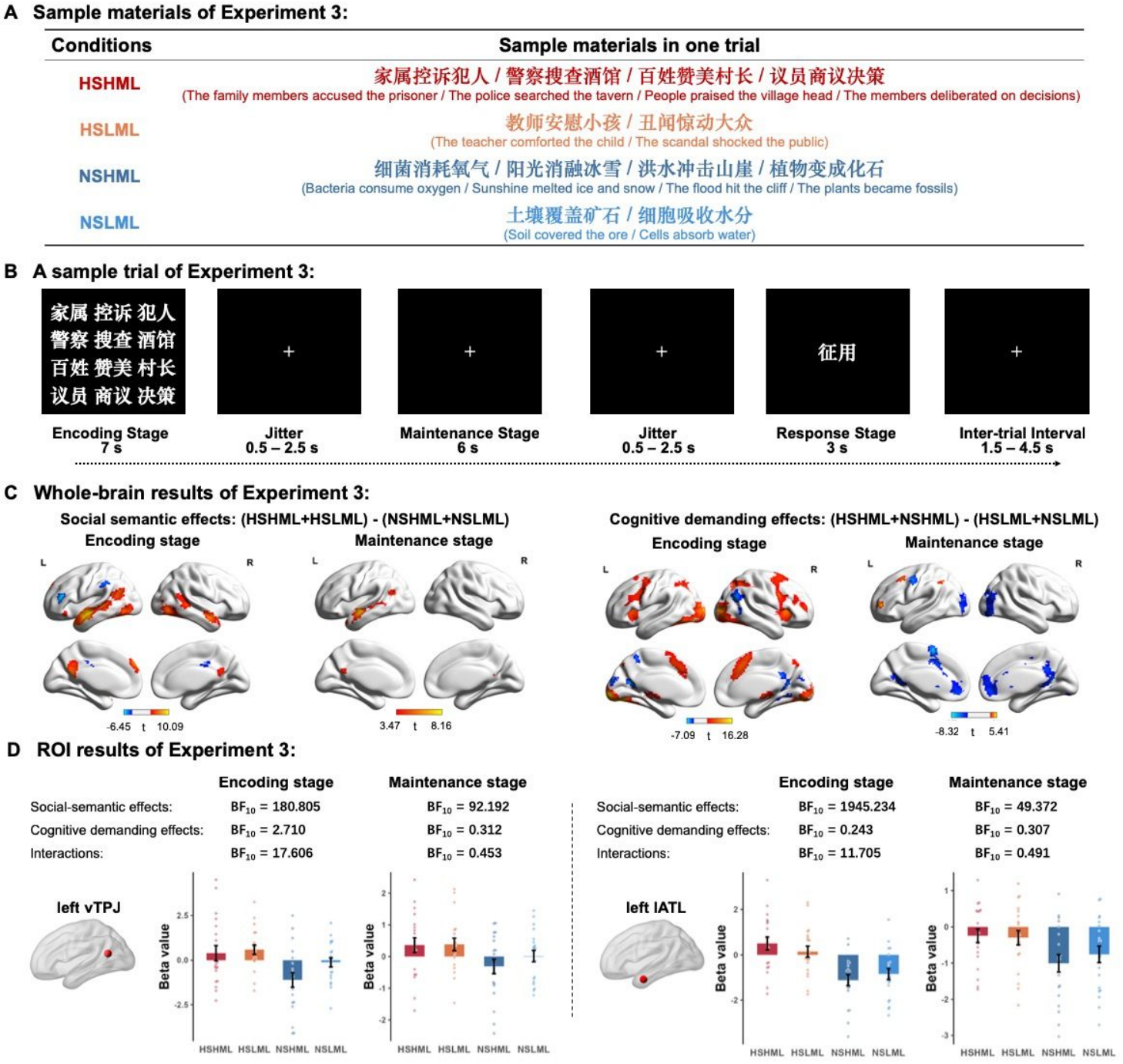

Figure 3

Persistent social-semantic-selective neural activity during the delay period (Experiment 3).

Panel A: The sample materials for each experimental condition. For each trial, the stimuli were two or four short sentences consisting of words of either high or no socialness. Slashes indicate the sentence boundaries.

Panel B: The trial structure of the task. In each trial, participants were asked to read and maintain the words. After a delay period, they performed a word recognition task.

Panel C: The whole-brain results (for more information on the results, see Table S4 and Table S5). The left vTPJ and lATL showed social-semantic activation in both encoding and maintenance stages, which is consistent with the key prediction of the social-semantic-working-memory hypothesis. Encoding more sentences invoked stronger activation in the core fronto-parietal working-memory network and visual cortex; maintaining more sentences invoked stronger activation in a few areas in the left lateral frontal and parietal cortex. Interaction between social-semantic and demanding effects was only found in the posterior cingulate and in the encoding stage, which is not shown in the figure (see Table S4).

Panel D: The ROI results (for the results of classical parametric tests, see Table S9). The bars show the mean beta values, the error bars show standard errors, and each point shows the data of a participant. As predicted by the social-semantic working memory hypothesis, in both ROIs, social-semantic effects were found in both encoding and maintenance stages. Interaction between social-semantic and demanding effects was found in both ROIs in the encoding but not maintenance stage.

Abbreviations: HSHML = high-socialness and high-memory-load, HSLML = high-socialness and low-memory-load, NSHML = nonsocial and high-memory-load, NSLML = nonsocial and low-memory-load.

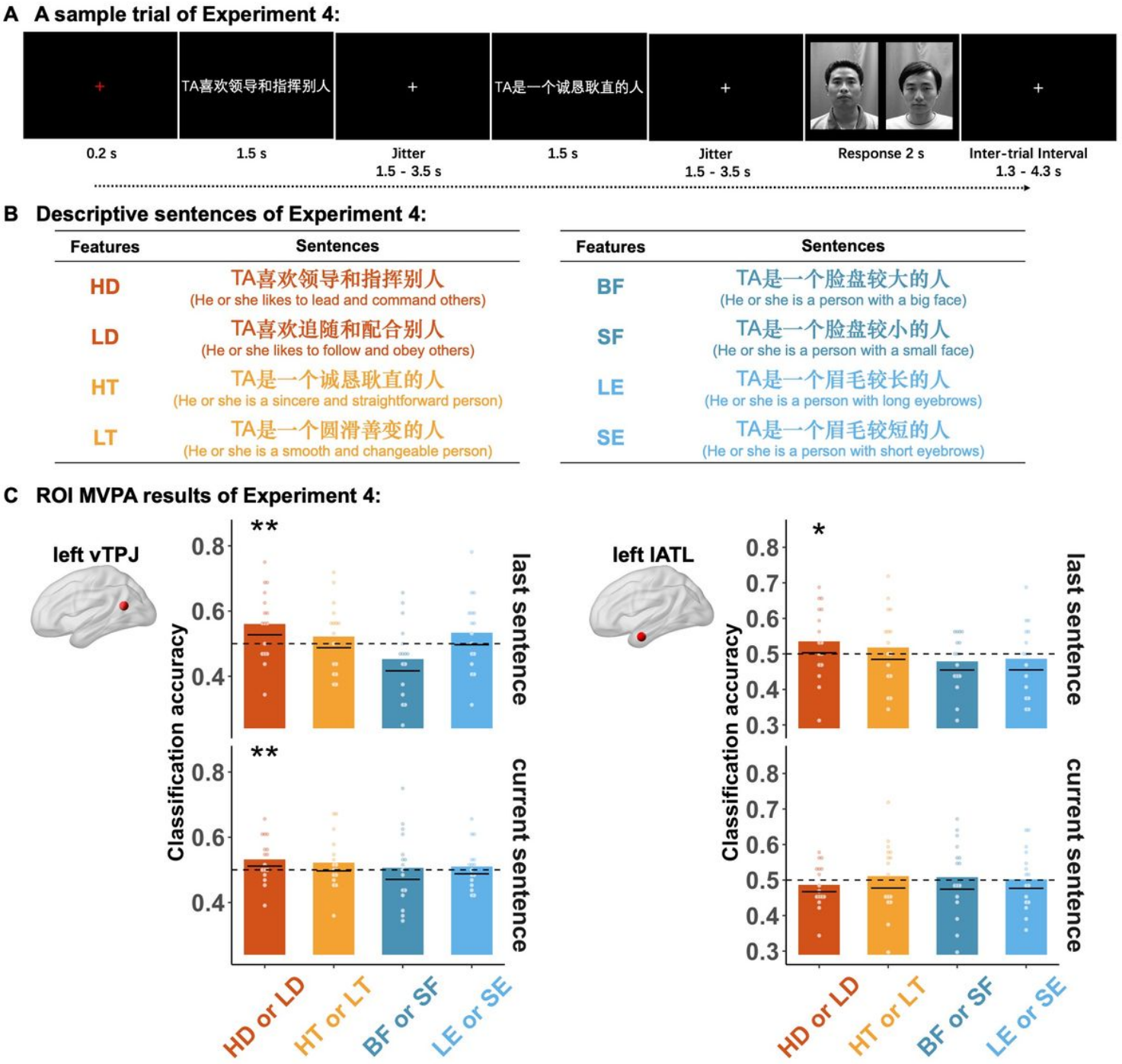

Figure 4

Persistent social-semantic-selective neural activity during the processing of successive sentences (Experiment 4).

Panel A: The trial structure of the task. In each trial, participants read two sentences describing either two trait features (dominance and trustworthiness) or two physical facial features (big/small face and long/short eyebrows) of a person. Then they were asked to choose a photograph from two to match the contents of the sentences.

Panel B: The descriptive sentences for each trait or physical facial dimension.

Panel C: The results of MVPA in ROIs. The bars show the averaged classification accuracies on the poles of the four dimensions described in the last (upper) and current sentences (lower). The black solid line in each bar shows the lower bound of 95% confidence interval for the classification accuracy obtained using bootstrap, and each point shows the data of a participant. The dashed line shows the change level (50%). In the left vTPJ, the features of dominance described in the current and last sentences can both be decoded from the activation patterns; in the left lATL, the features of dominance described in the last sentence can be decoded from the activation patterns, but the effect did not survive the Bonferroni correction for the number of dimensions decoded (N = 4). No other features can be decoded from the activation of the two ROIs.

Abbreviations: HD = high dominance, LD = low dominance, HT = high trustworthiness, LT = low trustworthiness, BF = big face, SF = small face, LE = long eyebrow, SE = short eyebrow.

Note. * p <.05, ** p <.01 (uncorrected).

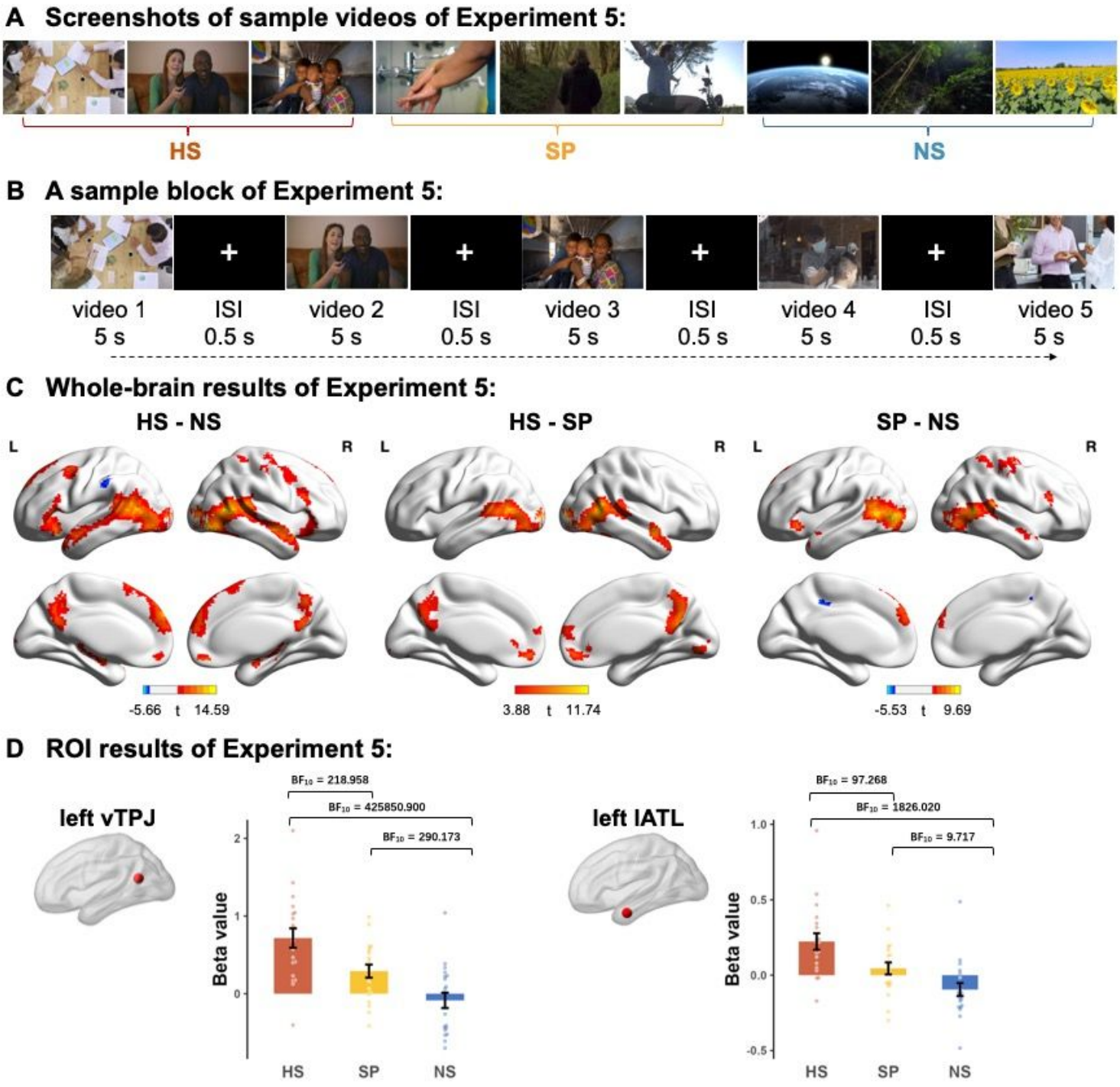

Figure 5

Left vTPJ and lATL are sensitive to the socialness of nonlinguistic stimuli (Experiment 5).

Panel A: Screenshots of sample videos of the high-socialness (left), single-person (middle), and nonsocial (right) conditions.

Panel B: The block structure. Each block contained 5 videos from the same condition.

Panel C: The whole-brain results (for more information on the results, see Table S6). The left vTPJ showed sensitivity to socialness in all contrasts between conditions (HS > SP > NS). The left lATL showed sensitivity to socialness in the contrast between HS and NS conditions.

Panel D: The ROI results (for the results of classical parametric tests, see Table S10). The bars show the mean beta values, the error bars show standard errors, and each point shows the data of a participant. Both ROIs showed sensitivity to socialness in all contrasts between conditions (HS > SP > NS).

Abbreviations: HS = high-socialness condition, SP = single-person condition, NS = nonsocial condition.

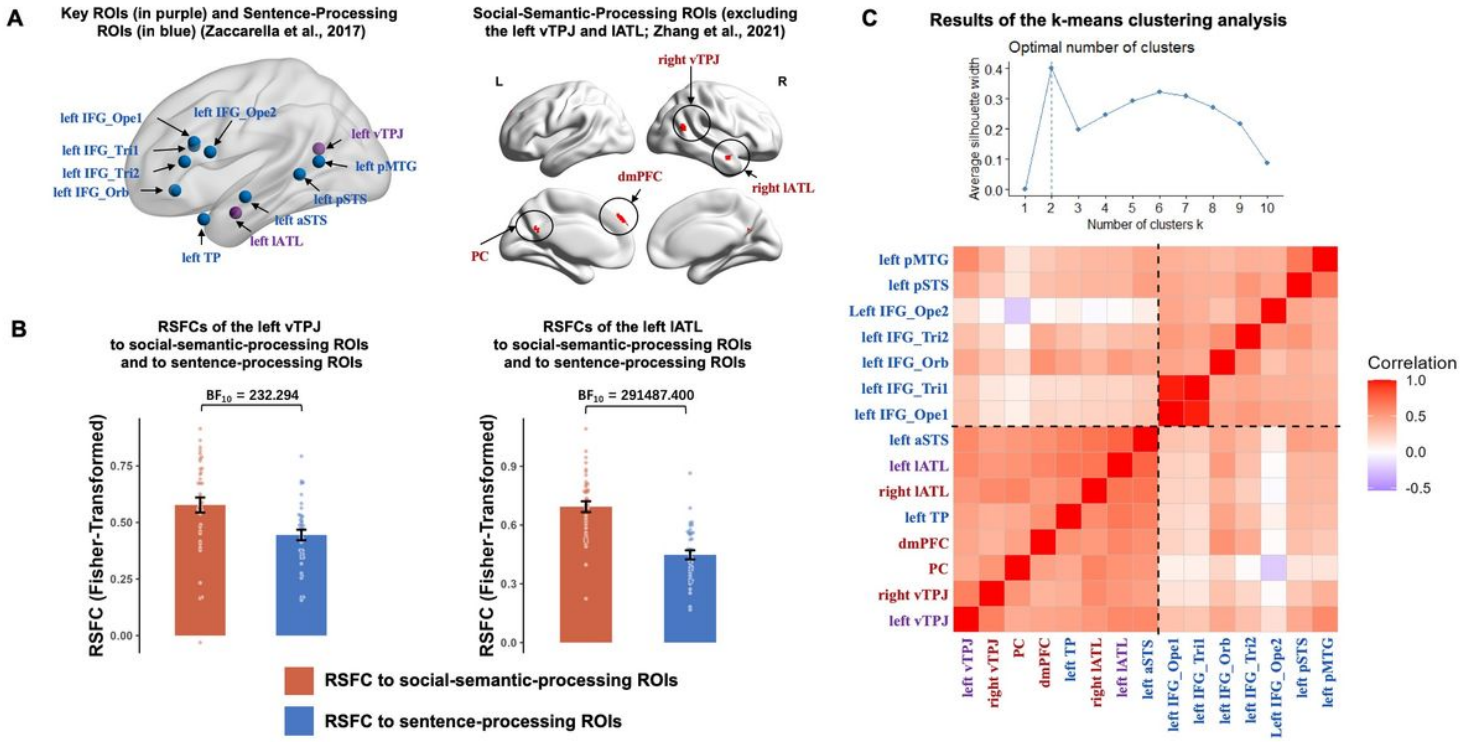

Figure 6

Left vTPJ and lATL have stronger intrinsic connectivity to the social-semantic-processing areas than to the sentence-processing areas (Experiment 6).

Panel A: The locations of the seed ROIs. The ROIs were defined based on two meta-analyses by Zaccarella et al. (2017) and Zhang et al. (2021). To remain consistent with the ROI analyses of Experiments 1 to 5, we defined the key ROIs (i.e. the left vTPJ and lATL) according to Zaccarella et al. (2017). The left vTPJ and lATL found in the meta-analysis of social-semantic-processing tasks (Zhang et al., 2021) were thus not included in the analysis. The sentence-processing ROIs and social-semantic-processing ROIs were defined according to Zaccarella et al. (2017) and Zhang et al. (2021), respectively. According to the prediction of the social-semantic-working-memory hypothesis, the left vTPJ and lATL should have stronger intrinsic connectivity to the social-semantic-processing ROIs than to the sentence-processing ROIs even they were defined based on sentence-processing tasks.

Panel B: Mean RSFCs of the key ROIs to social-semantic-processing and sentence-processing ROIs. For both the left vTPJ and lATL, their average RSFCs to the social-semantic-processing ROIs were stronger than those to the sentence-processing ROIs (for the results of classical parametric tests, see Table S11).

Panel C: The results of the k-means clustering analysis on all ROIs. The left vTPJ, lATL, aSTS and TP clustered together with the social-semantic-processing ROIs rather than the other sentence-processing ROIs, even they were defined based on the meta-analysis results of sentence-processing studies (Zaccarella et al., 2017). Upper: the averaged silhouette scores of the k-means clustering analysis. Lower: the best clustering solution shown by the dashed lines in the RSFC matrix of the seed ROIs.

Abbreviations: lFG_Orb = inferior frontal gyrus (orbital part), lFG_Ope = inferior frontal gyrus (opercular part), lFG_Tri = inferior frontal gyrus (triangular part), TP = temporal pole, aSTS = anterior superior temporal sulcus, pSTS = posterior superior temporal sulcus, pMTG = posterior middle temporal gyrus, PC = posterior cingulate.

Supplementary Files

This is a list of supplementary files associated with this preprint. Click to download.

- LinSupplementaryMaterialsNATHUMBEHAV23010347.docx